

# Light Curve Properties of Supernovae Associated With Gamma-ray Bursts

Xue Li and Jens Hjorth

Dark Cosmology Centre, Niels Bohr Institute, University of Copenhagen, Juliane Maries Vej 30, 2100, Copenhagen, Denmark,  
e-mail: lixue@dark-cosmology.dk

Received date/Accepted date

## ABSTRACT

*Context.* Little is known about the diversity in the light curves of supernovae (SNe) associated with gamma-ray bursts (GRBs), including whether the light curve of SN 1998bw can be used as a representative template or whether there is a luminosity-decline rate relation akin to that of SNe Ia.

*Aims.* In this paper, we aim to obtain well-constrained light curves of GRB-SNe without the assumption of empirical or parametric templates and to investigate whether the peak brightness correlates with other parameters such as the light curve shape or the time of peak.

*Methods.* We select eight SNe in the redshift range 0.0085 to 0.606, which are firmly associated with GRBs. The light curves of these GRB-SNe are well sampled across the peak. Afterglow and host galaxy contributions are subtracted and dust reddening is corrected for. Low-order polynomial functions are fitted to the light curves. A K-correction is applied to transform the light curves into the rest frame V band.

*Results.* GRB-SNe have fairly uniform peak luminosities, similar to SNe Ia. Moreover, GRB-SNe follow a luminosity-decline rate relation similar to the Phillips relation for SNe Ia. The relation between the peak magnitude  $M_{V,\text{peak}}$  and the decline rate  $\Delta m_{V,15}$  in V band is  $M_{V,\text{peak}} = 1.59^{+0.28}_{-0.24} \Delta m_{V,15} - 20.61^{+0.19}_{-0.22}$  mag, with  $\chi^2 = 5.2$  for 6 degrees of freedom. This luminosity-decline rate relation is tighter than the  $k - s$  relation, where  $k$  and  $s$  are the factors describing the relative brightness and width to the light curve of SN 1998bw. The peak luminosities of GRB-SNe are also weakly correlated with the time of peak: the brighter the GRB-SN, the longer the rise time.

*Conclusions.* The light curve of SN 1998bw, stretched around the time of explosion, can be used as a template for GRB-SNe with reasonable confidence, but stretching around the peak produces better results. GRB-SNe exhibit a luminosity-decline rate relation, similar to SNe Ia, both in normalization and slope. The existence of such a relation provides a new constraint on GRB explosion models. Considering the usefulness of SNe Ia in measuring cosmological distances, it is possible that GRB-SNe can be used as standardizable candles to measure cosmological distances and constrain cosmological parameters.

**Key words.** gamma-ray bursts: general — supernovae: general

## 1. Introduction

Gamma-ray bursts (GRBs) were first observed by the Vela Satellites in 1967 (Klebesadel et al. 1973). Being flashes of narrow beams of intense electromagnetic radiation observed in distant galaxies (Metzger et al. 1997) with peak energies in the gamma ray energy range, they are the most luminous phenomena in the universe. The bursts are usually separated into two classes: long and short (Kouveliotou et al. 1993). The long GRBs have a duration of more than two seconds, while the short events last less than two seconds. Since the first discovery of the connection between SN 1998bw and GRB 980425 (Galama et al. 1998; Iwamoto et al. 1998; Kulkarni et al. 1998; Woosley et al. 1999), many SNe have been found to be associated with long GRBs (Hjorth et al. 2003; Stanek et al. 2003; Woosley & Bloom 2006; Hjorth & Bloom 2012).

A collapsar model (MacFadyen & Woosley 1999; MacFadyen et al. 2001) has been developed to explain the GRB-SN connection. But the properties of GRB-SNe, as well as GRBs are still under debate, e.g., what are the progenitors for long and short GRBs? Can GRB-SNe be used as standard candles? To answer these and other relevant questions, light curves of GRB-SNe are required.

In previous studies, the light curves of SN 1998bw in the U, B, V, R, I bands were used as a template to model the light curves of GRB-SNe (Bloom et al. 1999; Ferrero et al. 2006; Cano 2013). The light curves of SN 1998bw were shifted to the corresponding redshift and scaled to the peak luminosity and stretched in time (Cano et al. 2011a). Some work used semi-analytical models (Richardson et al. 2006) to constrain GRB-SN light curves (Richardson 2009). But whether the semi-analytical models or the light curve of SN 1998bw can be used as a stretchable template is still unknown, not to mention if there is a better way to stretch the template other than stretching with factor  $s$  (Cano et al. 2011a). To test this, it is important to obtain light curves instead of using the SN 1998bw light curve as a template.

It is not easy to obtain light curves of GRB-SNe. Sometimes a GRB is so bright that even though its afterglow declines rapidly (van Paradijs et al. 1997), it may still exceed the brightness of its associated SN, in which case no SN will be detectable. This is also the case when a host galaxy is brighter than a GRB-SNe (Hjorth 2013). Dust along the line of sight will extinguish the SN light. Moreover, any constraint we impose on the light curves e.g., afterglow modeling or SN light curve modeling, may bias the study.

Our task is to find a way to obtain light curves of GRB-SNe without using light curve templates. With such light curves, we may test if peak luminosities of GRB-SNe are correlated with other properties of the light curves, such as is the case for SNe Ia (Phillips 1993; Riess et al. 1998; Phillips et al. 1999). We may further test if the light curve of SN 1998bw can be used as a general light curve template for GRB-SNe, and, if so, how to stretch this light curve template.

The outline of this paper is as follows. In section 2, we discuss the general steps in obtaining light curves of GRB-SNe from published data. In section 3, we present the data and obtain light curves for GRB-SNe. Then in section 4 we analyze the properties of the light curves of GRB-SNe. We present a luminosity-decline rate relation and other properties of the light curves for GRB-SNe. We also test if the light curve of SN 1998bw can be used as a general light curve template and if there is a better way to stretch it than the commonly used approach. In section 5, we summarize our investigation and discuss future prospects.

## 2. Light curves of GRB-SNe

Our goal is to obtain light curves of GRB-SNe in the rest frame V band. This is because, as shown in Figure 1, the spectral energy distribution (SED) peaks around the V band. In addition, the K-correction procedure (section 2.5) relies on using a redder band to correct to the rest-frame flux and we rely on the availability of suitable data. After the light curves are obtained, we measure peak magnitudes ( $M_{V,\text{peak}}$ ) and decline rates ( $\Delta m_{V,\alpha}$ ). Here  $\Delta m_{V,\alpha}$  is defined as the decline of the V-band magnitude  $\alpha$  days after the SN has reached its peak brightness.

For error estimation, we use a standard Monte Carlo method to resimulate the data throughout the paper. The resulting uncertainties are obtained as 68.3% ( $\pm 1\sigma$ ) of the total resimulated results. In general, to obtain a light curve, we account for the effects of the host galaxy and the afterglow, and subtract their contributions from the total flux. We correct for extinction and fit low-order polynomial functions to the resimulated data. A K-correction is used to get the peak magnitude and decline rate in the rest frame V band. To do so, we either apply a multi-band K-correction, or use the SN 1998bw peak SED and decay properties to correct the values of the peak magnitude and the decline rate in bands obtained in a wavelength close to the rest frame V band.

### 2.1. Host galaxy

The brightness observed is the total flux of the GRB-SN, the afterglow, and the host galaxy. In some cases, the host galaxy is sufficiently faint compared to the SN that the host contribution is negligible. But for other systems, the host galaxy will contaminate the SN light curve. In these cases, to obtain the intrinsic SN luminosity, the contribution of the host galaxy must be subtracted.

The brightness of a host galaxy is constant. It is usually observed when the SN has faded away. In this paper, we take the host brightness from the literature. The host brightness is resimulated with the standard Monte Carlo method, and subtracted from the total brightness.

### 2.2. Afterglow

Except for two long GRBs, i.e., GRB 060614 (Fynbo et al. 2006; Gal-Yam et al. 2006; Gehrels et al. 2006) and GRB 060505 (Fynbo et al. 2006; Ofek et al. 2007; McBreen et al. 2008), for which no associated SNe were detected, there are no other known cases of long duration GRBs for which the limits on detecting a SN rules out something that is about as bright as SN 1998bw (Hjorth & Bloom 2012).

GRBs are very luminous and energetic with isotropic energies up to  $E_{\gamma,\text{iso}} \sim 10^{54}$  erg (Hjorth & Bloom 2012; Xu et al. 2013). Soon after the burst, the flux of the GRB afterglow dominates the light, but it declines rapidly. In some cases, after a few days, the brightness of an afterglow will have decreased significantly and is no more a major contributor to the photometry. At this time, if the host galaxy is not brighter than the SN, usually we can observe the light from the SN.

We assume that the afterglow behaves as a power law or a broken power-law decay  $f(t) = c_1 t^{\beta_1}$  for  $t < t_{\text{break}}$  and  $f(t) = c_2 t^{\beta_2}$  for  $t \geq t_{\text{break}}$ , where  $f(t)$  is the flux of an afterglow,  $\beta_1$  and  $\beta_2$  are the decay slopes and  $t_{\text{break}}$  is the time for the change of the slopes from pre-break  $\beta_1$  to post-break  $\beta_2$ . We choose  $t_{\text{break}}$  based on the data or from the literature. This method is different from the broken power-law fits (Zeh et al. 2004; Cano et al. 2011b), but the effect is similar. The slopes, the break time for systems GRB 050525A and GRB 090618 (see section 3 for more discussion on each system) are listed in Table 1. The values of  $t_{\text{break}}$ ,  $\beta_1$  and  $\beta_2$  in the column of ‘smooth function’ are from the literature, while in the ‘broken power-law’ column, the value of  $\beta_2$  is used in this paper. When the results of the smooth function are fitted with a broken power-law way,  $\widehat{\beta}$  is the fitted post-break slope. Compare  $\widehat{\beta}$  and  $\beta_2$ , we conclude that the broken power-law fits is consistent with the results of broken power-law fits.

In this paper, we resimulate the afterglow data with the standard Monte Carlo method and fit the resimulated data with broken power-law functions. We remove the contribution of the afterglow by subtracting the fitted power-law functions.

### 2.3. Extinction, distance modulus, and rest frame time

Dust in galaxies reddens light emitted from GRB-SNe. There are two main contributing sources: dust in the host galaxy, where the GRB-SN is located, and dust in the Milky Way. In this paper, we take the values of host extinction, e.g.,  $A(V)_{\text{host}}$  or  $E(B - V)_{\text{host}}$ , from the literature. Schlafly & Finkbeiner (2011) found that the Galactic extinction is overestimated by DIRBE/IRAS dust map (Schlegel et al. 1998) and calculated the correction coefficients if the dust map is used. In this paper, with  $R_V = 3.1$ , we use the DIRBE/IRAS dust map (Schlegel et al. 1998) to get  $E(B - V)$ , then the coefficients (see Table 6 in Schlafly & Finkbeiner (2011)) are multiplied to correct the value.

The distance modulus is calculated and subtracted to obtain the absolute magnitude. In this paper, we adopt the cosmological parameters  $\{\Omega_m, \Omega_\Lambda\} = \{0.315, 0.685\}$  and  $H_0 = 67.3 \text{ km s}^{-1} \text{ Mpc}^{-1}$  in a flat universe (Planck Collaboration et al. 2013). The absolute magnitude is determined as

$$M = m - 5 \log_{10}(D_L/10\text{pc}) - \Delta K + 2.5 \log_{10}(1 + z), \quad (1)$$

where  $D_L$  denotes the luminosity distance and  $\Delta K$  represents the effect of the K-correction (section 2.5).

Peculiar velocities may affect the estimate of the distance modulus, especially for nearby SNe. Except for SN 1998bw which has peculiar velocity  $v_p = -90 \pm 70 \text{ km s}^{-1}$  (Li et al. 2014),

**Table 1.** The slopes and the break times for GRB 050525A and GRB 090618.

GRB/XRF/SN	smooth function <sup>a</sup>				broken power-law		reference
	$\bar{t}_{\text{break}}$ (day)	$\bar{\beta}_1$	$\bar{\beta}_2$	$\bar{\beta}^b$	$t_{\text{break}}$ (day)	$\beta_2$	
050525A/2005nc	0.3	1.1	1.8	1.63	0.3	$1.74^{+0.11}_{-0.15}$	(1), (2)
090618	$0.48 \pm 0.08$	$0.79 \pm 0.01$	$1.74 \pm 0.04$	$1.52^{+0.06}_{-0.05}$	0.5	$1.56^{+0.07}_{-0.08}$	(3)

<sup>a</sup>: An afterglow fitting method with  $m(t) = -2.5 \times \left( \left( \frac{t}{t_{\text{break}}} \right)^{\bar{\beta}_1} + \left( \frac{t}{t_{\text{break}}} \right)^{\bar{\beta}_2} \right)^{-1} + B$  (Cano et al. 2011b).

<sup>b</sup>: Post-break slope fitted to the smooth function with broken power-law method.

(1) Blustin et al. (2006), (2) Della Valle et al. (2006), (3) Cano et al. (2011b)

for the other systems we assume the peculiar velocity is 0 and the uncertainty is  $\delta v_p = 300 \text{ km s}^{-1}$  (Davis 2013). Therefore, the uncertainty in the distance modulus is  $(5/2.3) \delta v_p (cz)^{-1}$ , where  $c$  is the speed of light and  $z$  is the redshift of a GRB-SN.

It is straightforward to convert the observational time into the rest frame time by dividing the observational time by  $(1+z)$ .

#### 2.4. Polynomial function fitting

After the steps discussed above, polynomial functions are fitted to the data. We fit the data with the lowest possible order. The most suitable order is to some extent subjective, but as discussed below, in most cases the polynomial functions are of 3rd or 4th order. Data on both sides of the peak are needed. This is to ensure that parameters dependent on sampling the peak, such as the time of peak, the peak brightness, and the decline rate past peak, are robustly determined.

#### 2.5. K-correction

The observational data of GRB-SNe may be in U, B, V, R, I and other bands. After subtracting the host and afterglow brightness and fitting polynomial functions to the results, light curves of SNe are obtained in the observed bands. Then a K-correction is applied to correct light curves from the observed band(s) into the rest frame V band. If the systems have been observed in two or more bands and two bands are close to the redshifted V band for interpolation, then a ‘multi-band K-correction’ (van Dokkum & Franx 1996; Hogg et al. 2002) is applied. For the other systems, which have data in only one band or the other bands are not close to the redshifted V band, we correct their peak magnitude and decline rate with peak SED and decline rate templates based on SN 1998bw. We use broad-band data because we do not have useful spectra around (before and after) the peak of the light curve.

##### 2.5.1. Multi-band K-correction

The multi-band K-correction is a method to constrain the light curves in the rest frame V band by interpolating two light curves in adjacent observed bands (van Dokkum & Franx 1996; Hogg et al. 2002). The method is based on the assumption that flux densities are correlated in contiguous bands. For example, if a GRB-SNe has  $z \in (0.26, 0.60)$ , then we can interpolate the magnitude in the R and I bands into the redshifted V band. The flux density in the V band can be estimated as:  $F(v_V(z)) = F(v_R)^c F(v_I)^{1-c}$ . The magnitude in the redshifted V band is then

$$V_z = cR + (1-c)I, \quad (2)$$

where  $V_z$ ,  $R$  and  $I$  are magnitudes in the AB system. The parameter  $c$  is calculated as a function of central wavelength of the observed bands and the SN redshift (van Dokkum & Franx 1996). Here  $c = (\lambda_I - \lambda_V(1+z))/(\lambda_I - \lambda_R)$  with  $\lambda_R$  and  $\lambda_I$  being the observational R and I band wavelengths and  $\lambda_V(1+z)$  being the redshifted V band wavelength. In this step, the selected two bands should fulfill the conditions: 1) the two bands must be adjacent; 2) the parameter should be  $c \in (0, 1)$  to make sure one is not extrapolating beyond the observed bands.

##### 2.5.2. SN 1998bw peak SED and decline rate templates

When useful light curve data is available only in one band, or the other observed bands are too far away from the redshifted V band to do a meaningful multi-band K-correction, we resort to using the light curves of SN 1998bw as a template to obtain V-band values from data close to the redshifted V band, typically within a few hundred Å. The observed band which is closest to the redshifted V band is chosen to obtain the light curves and measure the values of the peak magnitude and the decline rate. After that, according to the wavelength of the chosen band,  $M_{V,\text{peak}}$  and  $\Delta m_{V,\alpha}$  are corrected to the rest frame V band using the light curves of SN 1998bw as a template.

The SN 1998bw peak SED and decline rate templates describe the relations of  $M_{\text{peak}}$  and  $\Delta m_{\text{alpha}}$ , as a function of wavelength  $\lambda$ . It is based on the assumption that the behavior of the light curves in different bands are similar for all GRB-SNe. Compared to other effects, e.g., extinction, host and afterglow subtraction, this is a 2nd order effect and does not require that the overall light curves or spectra are perfectly identical to those of SN 1998bw.

Here we use the observational data of SN 1998bw (Galama et al. 1998; Clocchiatti et al. 2011; Sollerman et al. 2002) to establish the template (see section 3.1 for details on SN 1998bw). The light curves are well defined by the observational data. Therefore, peak magnitudes  $M_{\text{peak}}$  and the decline rates  $\Delta m_{\alpha}$  are constrained in the U, B, V, R, I bands. Then we spline interpolate the relations between  $M_{\text{peak}}$ ,  $\Delta m_{\alpha}$  and  $\lambda$ . The resulting templates are shown in Figure 1. The peak magnitude is corrected as  $M_{V,\text{peak}} = M_{\lambda}^{\text{data}} - M_{\lambda}^{\text{temp}} + M_V^{\text{temp}}$ , where  $M_{\lambda}^{\text{data}}$  represents the peak magnitude at the wavelength  $\lambda = \lambda_{\text{obs}}/(1+z)$ , with  $\lambda_{\text{obs}}$  being the observational wavelength, while  $M_{\lambda}^{\text{temp}}$  and  $M_V^{\text{temp}}$  denote the measured values at the wavelength  $\lambda$  and in the V band respectively, obtained from the SN 1998bw peak SED and decline rate templates. The decline rate  $\Delta m_{V,\alpha}$  is corrected in the same way.

The differences of  $M_{V,\text{peak}}$  estimated via the two methods of K-correction are shown in Figure 2 for four systems: SN 1998bw, SN 2006aj, SN 2010bh and SN 2012bz (see section

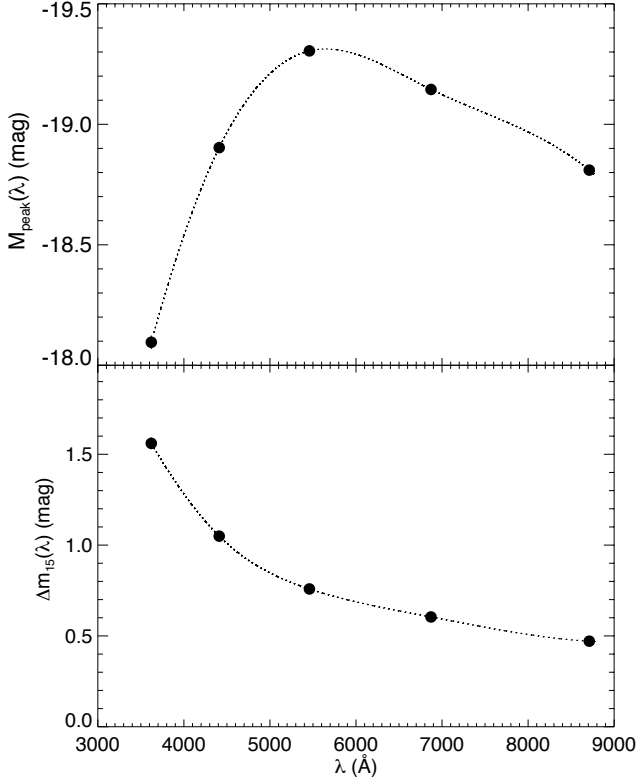


**Fig. 1.** SN 1998bw peak SED and decline rate templates. The black points represent values in the U, B, V, R, I bands (Galama et al. 1998; Clocchiatti et al. 2011; Sollerman et al. 2002). The dotted lines are spline interpolations. The upper panel shows the relation between the wavelength  $\lambda$  and the peak magnitude  $M_{\text{peak}}(\lambda)$ . In the lower panel, the relation between the wavelength  $\lambda$  and the decline rate  $\Delta m_{\alpha}(\lambda)$  is plotted. Here we show values for  $\alpha = 15$ .  $M_{\text{peak}}$  values have errors  $< 0.02$  mag while  $\Delta m_{15}$  values have errors  $< 0.026$  mag in the V, R and I bands.

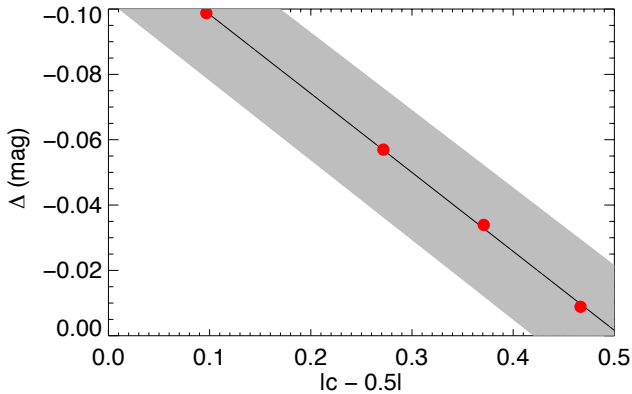


**Fig. 2.** Difference of peak magnitude ( $\Delta$ ) estimated via two K corrections as a function of K-correction factor  $c$  (Eqs. 2 and 3). We show the results for four systems: SN 1998bw, SN 2006aj, SN 2010bh and SN 2012bz (see section 3 for details). The shaded area shows the systematic uncertainty of 0.02 mag in the K correction procedure.

3 for more discussion on each system). Here  $|c - 0.5|$  represents the relative distance of the redshifted V band wavelength to the average of two observed wavelengths. The differences between the two methods may get bigger as the redshifted V band is closer to the middle point of two observed bands. Here  $\Delta = M_{\text{V,peak}}^{\text{temp}} - M_{\text{V,peak}}^{\text{multi}}$ , where  $M_{\text{V,peak}}^{\text{temp}}$  denotes the peak magnitude estimated via the SN 1998bw peak SED and decline rate template and  $M_{\text{V,peak}}^{\text{multi}}$  is the value obtained from the multi-band K-correction. A linear fit to the relation gives

$$\Delta = 0.24 \cdot |c - 0.5| - 0.12. \quad (3)$$

Figure 2 shows that two methods lead to small differences with  $|\Delta| \leq 0.1$  mag. The peak of  $M_{\text{peak}}(\lambda)$  on the SN 1998bw peak SED and decline rate templates is around 5500  $\text{\AA}$ , which is close to the V band. Therefore, the multi-band K-correction, obtained by interpolating magnitudes on each side of the peak, may underestimate the value of  $M_{\text{V,peak}}$ . We therefore apply the modification (Eq. 3) to the multi-band K-correction. We adopt a systematic uncertainty of 0.02 mag in quadrature in the K correction after applying this modification, as shown in the shaded area in Figure 2.

### 3. Systems of GRB-SNe

Based on the degree of observational evidence of a GRB having an associated SN (Hjorth & Bloom 2012), GRB-SNe are graded from class A to class E, where class A has ‘strongest spectroscopic evidence’, while class E has the weakest evidence. In this paper, we select GRB-SN candidates in classes A, B, and C. In total 19 systems are collected (see Table 9.1 in Hjorth & Bloom 2012), including SN 2012bz (Schulze et al. 2014) which is classified as a class A system.

We have studied all the 19 GRB-SN systems and evaluated the feasibility of constraining model-independent peak magnitudes and decline rates for them. Among them, we succeed to measure  $M_{\text{V,peak}}$  and  $\Delta m_{\text{V},\alpha}$  for 8 systems, as listed in Table 2, along with the corrections made in each case. We address the other systems and the reasons why they are not selected in section 3.9.

#### 3.1. GRB 980425/SN 1998bw

SN 1998bw was the first SN discovered to be connected with a GRB, GRB 980425 (Galama et al. 1998). Combined with the peculiar velocity  $v_p = -90 \pm 70 \text{ km s}^{-1}$  (Li et al. 2014) and the CMB velocity  $v_{\text{CMB}} = 2505 \pm 14 \text{ km s}^{-1}$  (Fixsen et al. 1996), it has  $v_z = 2595 \pm 71 \text{ km s}^{-1}$ . The redshift is  $z = v_z/c = 0.00866 \pm 0.00024$ . It is by far the lowest redshift of GRB-SNe. A lot of work have been done on this system, which is why we have built the peak SED and decline rate templates based on this system. This system is a class A GRB-SNe.

We collect the data in the V and R bands (Galama et al. 1998; Sollerman et al. 2002; Clocchiatti et al. 2011). We assume that the host galaxy and afterglow contributions to the total brightness are negligible and fit 4th order polynomials to the light curves. We have enough data in the V and R bands and these two bands are close to the redshifted V band, so the multi-band K-correction is applied. The parameter in the K-correction is  $c = 0.97$ . We assume that the host extinction is negligible. Unless stated otherwise, we treat GRB-SNe in the same way and neglect the contributions from the host galaxy, the afterglow or the host extinction, if they are not mentioned in the literature.

**Table 2.** The selected systems and the relevant steps.

GRB/XRF/SN	afterglow <sup>a</sup>	host <sup>b</sup>	k/t <sup>c</sup>	class	reference
980425/1998bw	-	-	<i>k</i>	<i>A</i>	(1), (2), (3)
030329/2003dh	-	-	<i>t</i>	<i>A</i>	(4), (5)
031203/2003lw	-	√	<i>t</i>	<i>A</i>	(6), (7), (8)
050525A/2005nc	√	√	<i>t</i>	<i>B</i>	(9), (10)
060218/2006aj	-	√	<i>k</i>	<i>A</i>	(11), (12), (13), (14), (15)
090618	√	√	<i>t</i>	<i>C</i>	(16)
100316D/2010bh	-	-	<i>k</i>	<i>A</i>	(17), (18), (19)
120422A/2012bz	√	-	<i>k</i>	<i>A</i>	(20), (21)

<sup>a</sup>: Subtraction of afterglow brightness.

<sup>b</sup>: Subtraction of host galaxy brightness.

<sup>c</sup>: Multi-band K-correction (denoted ‘*k*’) or shift based on the SN 1998bw peak SED and decline rate templates (denoted ‘*t*’).

(1) Galama et al. (1998), (2) Sollerman et al. (2002), (3) Clocchiatti et al. (2011), (4) Hjorth et al. (2003), (5) Matheson et al. (2003), (6) Malesani et al. (2004), (7) Mazzali et al. (2006), (8) Malesani (2013), (9) Blustin et al. (2006), (10) Della Valle et al. (2006), (11) Sollerman et al. (2006), (12) Ferrero et al. (2006), (13) Šimon et al. (2010), (14) Guenther et al. (2006), (15) Poznanski et al. (2012), (16) Cano et al. (2011b), (17) Cano et al. (2011a), (18) Olivares E. et al. (2012), (19) Bufano et al. (2012), (20) Melandri et al. (2012), (21) Schulze et al. (2014).

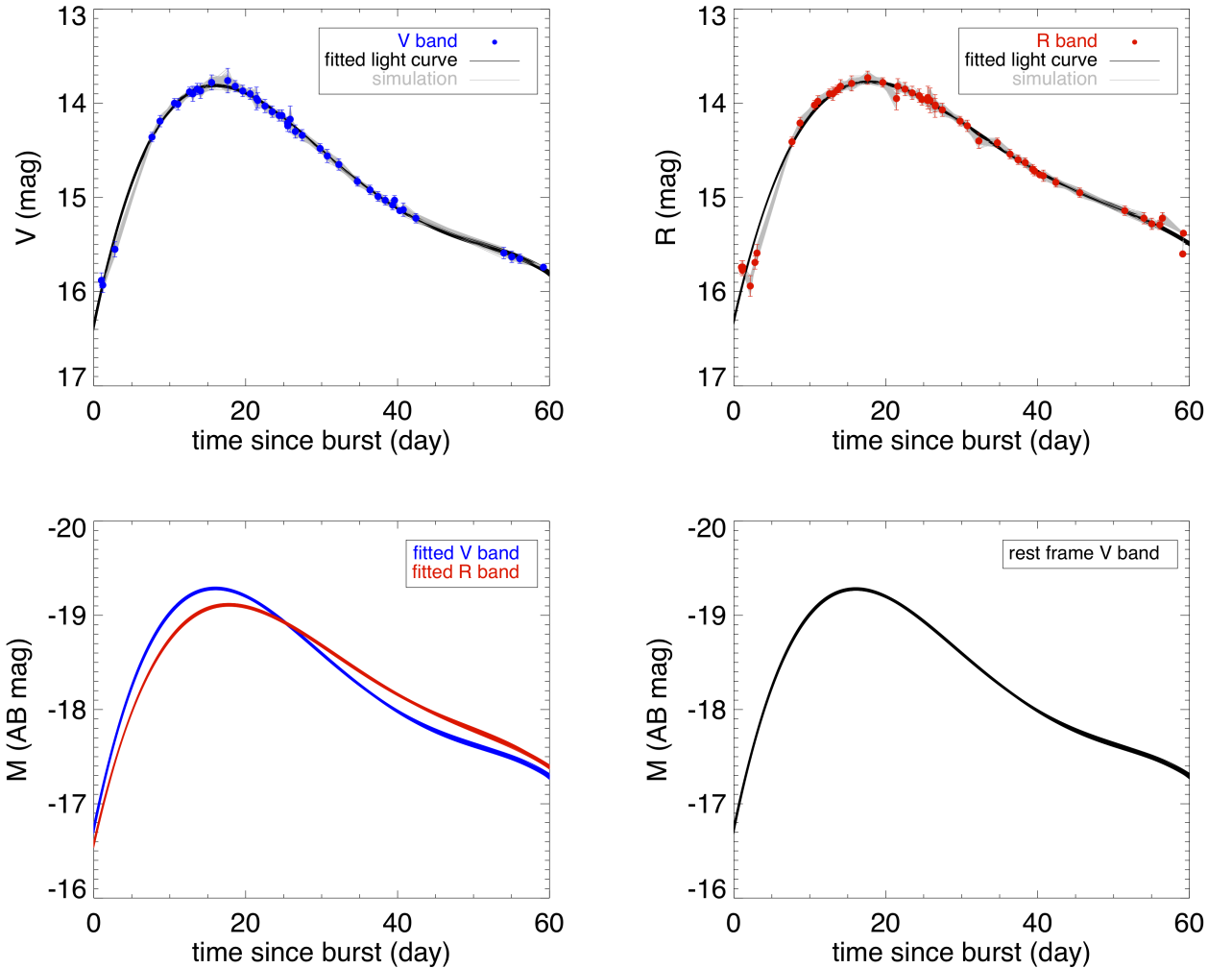


**Fig. 3.** GRB 980425/SN 1998bw. The upper panels show the photometric data points (blue/red), the resimulated data (gray) and the polynomial functions fitted to the resimulated data in V (*left*) and R (*right*) bands. In the lower left panel, the light curves after the extinction and the distance modulus correction are plotted in V band (blue) and R band (red) in AB magnitude. In the lower right panel, the final light curves after the K-correction in the rest frame V band are plotted. The uncertainties in the resimulated data and the fitting light curves are plotted as 68.3% ( $\pm 1\sigma$ ) of the total resimulated results.

The Galactic extinction is estimated to be  $E(B - V) = 0.06$  mag. The distance modulus is  $\mu = 32.94 \pm 0.08$ . The uncertainty in the distance modulus is dominated by the uncertainty in the peculiar velocity.

Figure 3 shows the light curves of SN 1998bw. In the upper panel, the observational data, the resimulated data and the fitting functions to the resimulated data in the V (left) and R (right) bands are plotted. In the lower panel, the left plot shows the light curves in the V and R bands, after correcting for the Galactic extinction and converting into the absolute magnitude. On the right, after the K-correction, the light curves in the rest frame V band are plotted. The temporal axes in the four panels have been corrected into the rest frame. The uncertainties in the resimulated data and the fitting light curves are plotted as 68.3% ( $\pm 1\sigma$ ) of the total resimulated results. In this section, the similar figures show 100 out of the 1000 resimulated light curves.

### 3.2. GRB 030329/SN 2003dh

The GRB 030329/SN 2003dh system was the first solid spectroscopic association between a cosmological GRB and a SN (Hjorth et al. 2003; Stanek et al. 2003). The redshift is  $z = 0.1685$ . It is a class A system. The data is collected in the V band (Hjorth et al. 2003). With an SMC extinction law, Matheson et al. (2003) estimated the host extinction to be  $A_{V,\text{host}} = 0.12 \pm 0.22$  mag. We assume no host extinction, which is consistent with the result from Matheson et al. (2003). The Galactic extinction is  $E(B - V)_{\text{MW}} = 0.025$  mag and the distance modulus is  $\mu = 39.63 \pm 0.01$ . Due to the small number of data points, we fit 2nd order polynomial functions to the resimulated data. The  $M_{V,\text{peak}}$  and  $\Delta m_{V,15}$  for this system are corrected with the SN 1998bw peak SED and decline rate templates. The results are shown in Figure 4 (left).

### 3.3. GRB 031203/SN 2003lw

GRB 031203 (SN 2003lw) had a very faint afterglow and a relatively bright host galaxy with  $V_{\text{host}} = 20.57 \pm 0.05$  mag and  $R_{\text{host}} = 20.44 \pm 0.02$  mag (Mazzali et al. 2006; Malesani 2013). It is a class A system.

The redshift is  $z = 0.1055 \pm 0.0001$  (Prochaska et al. 2004). We collect data in the V and R bands (Malesani et al. 2004; Mazzali et al. 2006).

The observed fluxes are corrected for the significant host contribution. After that, we fit 2nd order polynomial functions to the resimulated data. Unfortunately, the V band data do not cover the rising part of the light curve. Therefore, only the R band data is used to generate the light curves. This system has uncertain extinction. From Prochaska et al. (2004), a lower Galactic extinction is adopted to be  $E(B - V)_{\text{MW}} = 0.78$  mag, and total extinction is  $E(B - V)_{\text{total}} = 1.17 \pm 0.1$  mag, through Balmer line ratio study. Through spectral modeling, (Mazzali et al. 2006) favors a value of the host extinction  $E(B - V)_{\text{host}} = 0.25$  mag and  $A_{V,\text{host}} = 0.78 \pm 0.16$  mag (Cardelli et al. 1989) and total reddening  $E(B - V)_{\text{total}} \sim 1.07 \pm 0.05$  mag. We adopt the Galactic extinction to be  $E(B - V)_{\text{MW}} = 1.06$  mag and the host extinction to be  $A_{V,\text{host}} = 0.78 \pm 0.16$  mag from Mazzali et al. (2006). We consider the peak magnitudes are uncertain values, because the host extinction is uncertain. The distance modulus is  $\mu = 38.52 \pm 0.02$ . The  $M_{V,\text{peak}}$  and  $\Delta m_{V,15}$  for this system are corrected with the SN 1998bw peak SED and decline rate templates. The results are shown in Figure 4 (right).

### 3.4. GRB 050525A/SN 2005nc

GRB 050525A (SN 2005nc) is a long GRB with redshift  $z = 0.606$  (Blustin et al. 2006). It is a class B system.

We collect data from Della Valle et al. (2006). Only R band data is available. Therefore, the SN 1998bw peak SED and decline rate templates are applied. We subtract the host contribution with  $R_{\text{host}} = 25.2 \pm 0.1$  mag (Della Valle et al. 2006). Then we resimulate and subtract the afterglow data, fitted as a broken power-law, to get the intrinsic SN flux. After that, we fit 3rd order polynomial functions to the resimulated data. The host extinction is estimated to be  $A_{V,\text{host}} = 0.26 \pm 0.12$  mag (Cardelli et al. 1989; Pei 1992; Blustin et al. 2006), assuming an SMC extinction curve. For the Galactic extinction, the foreground extinction is  $E(B - V)_{\text{MW}} = 0.094$  mag. The distance modulus is  $\mu = 42.84 \pm 0.004$ . Figure 5 (left) shows the results for SN 2005nc.

### 3.5. XRF 060218/SN 2006aj

The X-Ray Flash (XRF; Heise et al. 2001) 060218 is a long GRB. The redshift is  $z = 0.03342$ . This system is another class A GRB-SN.

We collect data from Sollerman et al. (2006), Ferrero et al. (2006), and Šimon et al. (2010) in the V and R bands. SN 2006aj is an extreme case (Šimon et al. 2010) because before a normal SN peak, there is an early peak and these two peaks are equally bright. The data from Šimon et al. (2010) includes the early part ( $< 2.5$  days) of the photometry since the burst, therefore the light curve shows two bumps. In this paper, we study the normal SN light curve so we only collect the data after 2.5 days since the burst.

SN 2006aj is located in a relatively bright host galaxy with  $V_{\text{host}} = 20.19 \pm 0.04$  mag and  $R_{\text{host}} = 19.86 \pm 0.03$  mag (Sollerman et al. 2006), which are subtracted from the observed fluxes. The distance modulus is  $\mu = 35.92 \pm 0.07$ . We fit 4th order polynomial functions. There is a discrepancy in the reported estimates of the host extinction. Campana et al. (2006) estimate it to be  $E(B - V)_{\text{host}} = 0.2 \pm 0.03$  mag, assuming an SMC reddening law. Assuming the relation between sodium absorption and dust extinction from Munari & Zwitter (1997) is representative for interstellar medium, Guenther et al. (2006) find  $E(B - V)_{\text{host}} = 0.042 \pm 0.003$  mag. With an updated empirical relation from Poznanski et al. (2012), the extinctions are  $E(B - V)_{\text{host}} = 0.026 \pm 0.014$  mag and  $E(B - V)_{\text{MW}} = 0.061 \pm 0.03$  mag, which are about half of the values from Munari & Zwitter (1997). We adopt the Galactic extinction is  $E(B - V)_{\text{MW}} = 0.145$  mag. The host extinction is estimated to be  $E(B - V)_{\text{host}} = 0.026 \pm 0.014$  mag and  $A_{V,\text{host}} = 0.076 \pm 0.041$  mag with the updated empirical relation from Poznanski et al. (2012). We apply the multi-band K-correction with  $c = 0.87$ . Figure 6 shows the light curves of SN 2006aj.

### 3.6. GRB 090618

The long GRB 090618 is a class C system with  $z = 0.54$  (Cano et al. 2011b). We collect data from Cano et al. (2011b) in the i band. We subtract the brightness of the host galaxy and the afterglow. The host brightness is estimated to be  $i_{\text{host}} = 23.22 \pm 0.06$  mag (Cano et al. 2011b). The afterglow is fitted with broken power-law functions and the resimulated data are fitted with 3rd order polynomial functions. The Galactic extinction is  $E(B - V)_{\text{MW}} = 0.09$  mag. From X-ray to optical SED fitting, the host extinction is  $A_{V,\text{host}} = 0.3 \pm 0.1$  mag according to Cano et al.

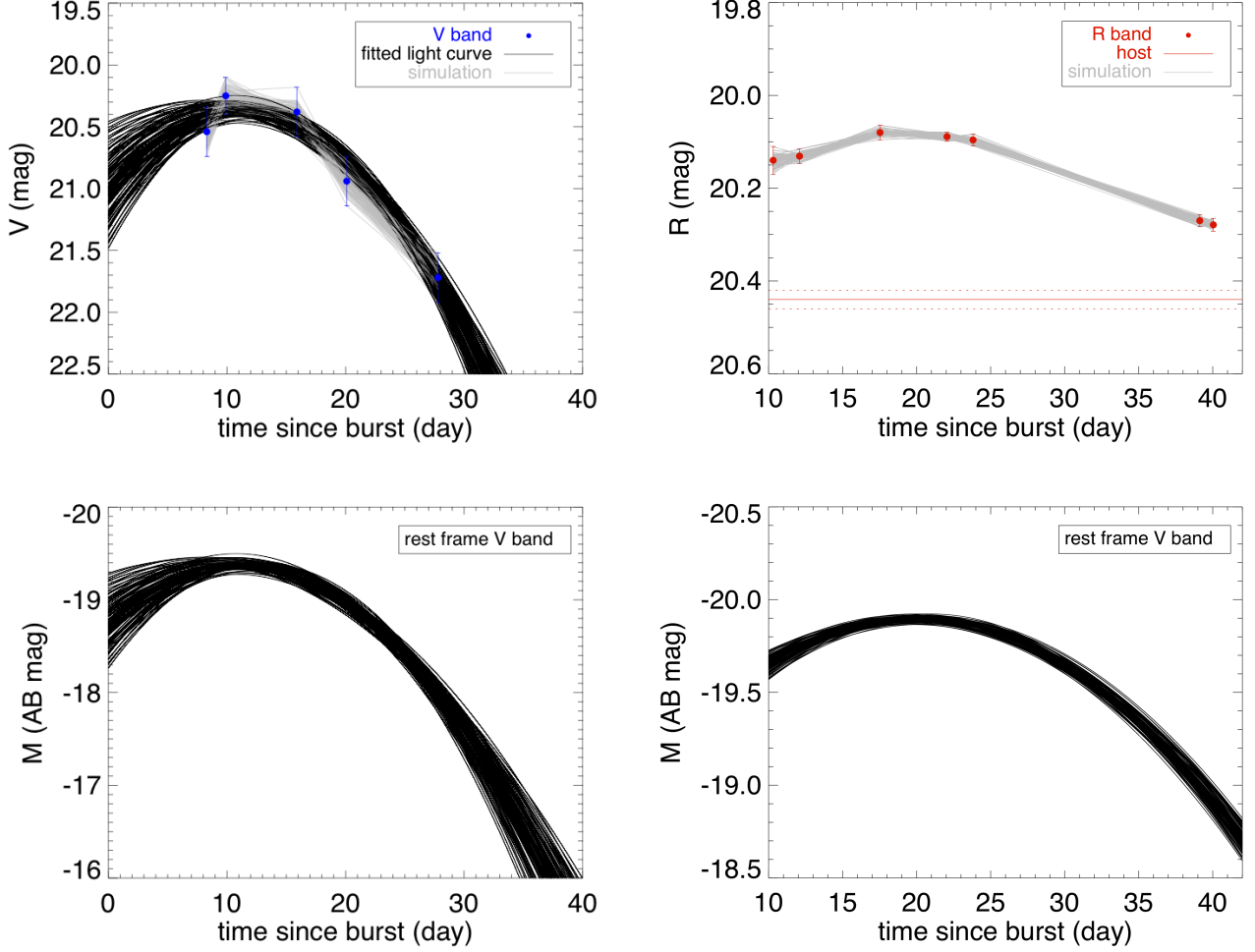


**Fig. 4.** GRB 030329/SN 2003dh (*left*) and GRB 031203/SN 2003lw (*right*). The line styles are the same as in Figure 3.

(2011b). The distance modulus is  $\mu = 42.54 \pm 0.004$ . The SN 1998bw peak SED and decline rate templates are used to convert the peak magnitude and the decline rates into the rest frame V band. Figure 5 (right) shows the results for GRB 090618.

### 3.7. XRF 100316D/SN 2010bh

XRF 100316D is a soft long GRB (Cano et al. 2011a). It is a class A system. The redshift is  $z = 0.059$  and we use published photometry in the V and R bands (Cano et al. 2011a; Olivares E. et al. 2012; Bufano et al. 2012). The three data sets are not consistent with each other (shown in Figure 7). There are systematic offsets in the photometry, especially around the peak. Compared to Bufano et al. (2012) and Cano et al. (2011a), the R band data from Olivares E. et al. (2012) is about 0.3 mag fainter at the peak. This may be because of zero point discrepancies. We reduce the offset by subtracting 0.3 mag from the R band data (Olivares E. et al. 2012), although we acknowledge there is a possibility that the other two data sets should be shifted instead.

The foreground extinction is  $E(B - V)_{\text{MW}} = 0.117$  mag. Reported values of the host extinction are very different. Using the  $H\alpha/H\beta$  ratio, the host extinction is estimated to be  $E(B - V)_{\text{host}} = 0.14$  mag (Bufano et al. 2012). From color excess measurement, Cano et al. (2011a) assumes the host extinction to be  $E(B - V)_{\text{host}} = 0.18 \pm 0.08$  mag. Olivares E. et al. (2012)

estimated the extinction using afterglow SED fitting and found  $A_{V,\text{host}} = 1.20 \pm 0.09$  mag. We adopt this value because the intrinsic SN spectrum is otherwise very red (Levan et al. (2013)). However, we consider the peak magnitude an uncertain value because of the possible zero point errors in the photometry and the uncertain extinction correction.

The distance modulus is  $\mu = 37.20 \pm 0.04$ . We fit 4th order polynomial functions to the resimulated data. The multi-band K correction parameter is  $c = 0.77$ . Figure 7 shows the resulting light curves for SN 2010bh.

### 3.8. GRB 120422A/SN 2012bz

Extensive observations have been done to detect GRB 120422A (SN 2012bz) with telescopes from mm to optical wavelengths (Melandri et al. 2012; Schulze et al. 2014). It is a class A system.

The redshift is  $z = 0.283$ , and the data are collected from Melandri et al. (2012); Schulze et al. (2014) in the  $r'$  and  $i'$  bands. Compared to the X-ray lightcurve (Fig. 2 in Schulze et al. (2014)), the afterglow in the  $r'$  and  $i'$  bands have a significant supernova contribution, so we fix the post-break slope  $\beta = 1.48 \pm 0.4$  based on the X-ray observations (Schulze et al. 2014). But the subtraction of the afterglow barely changes the intrinsic SN brightness. So for this system, either we fix the slope based on X-ray observation or on the SN modeling have no dif-

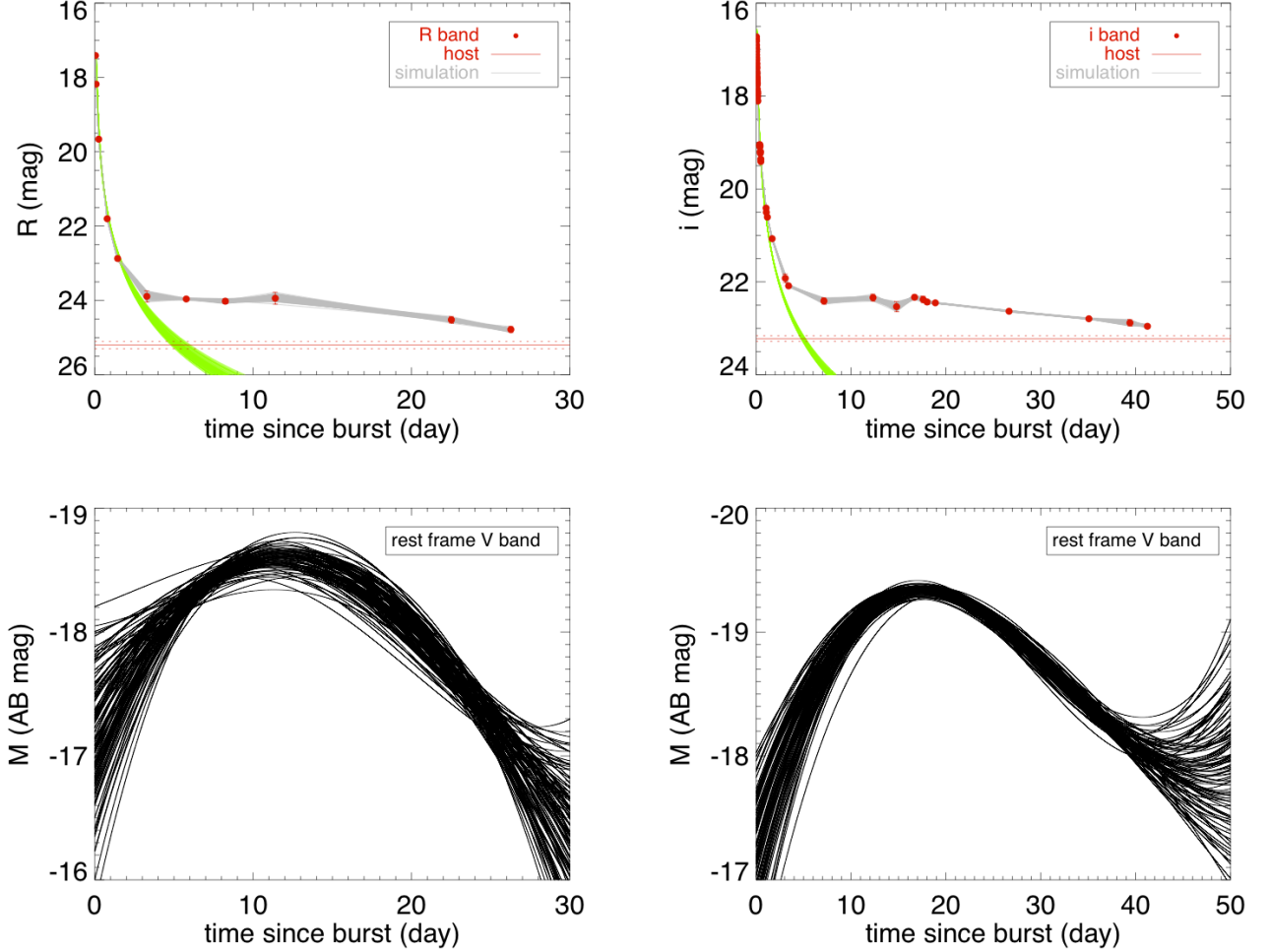


**Fig. 5.** GRB 050525A /SN 2005nc (left) and GRB 090618 (right). The line styles are the same as in Figure 3. The green lines are the broken power-law functions fitted to the afterglow.

ference to the brightness of the SN (Schulze et al. 2014). We adopt the foreground extinction to be  $E(B - V)_{\text{MW}} = 0.035$  mag. The resimulated data are fitted with 4th order polynomial functions. The distance modulus is  $\mu = 40.89 \pm 0.01$ . The multi-band K-correction parameter is  $c = 0.40$ . Figure 8 shows the light curve results.

### 3.9. GRBs not included

We investigated the possibilities of obtaining light curves for other GRB-SNe in class *A*, *B* and *C*. Here we briefly explain the reasons why we do not report the light curves for these systems.

There are several reasons that may cause the failure of obtaining the light curves in the rest frame V band: 1) The errors in the subtraction of the afterglow will inflate the errors in the SN photometry. This is a major reason why for some systems, even though enough data points have been obtained, after the afterglow fitting, there are too few useful data points left to do the polynomial fitting. We cannot get full light curves (notably information at and before the peak) for these systems. 2) Some systems lack data in proper band(s) to do the K-correction. This is because the multi-band K-correction is only valid when the redshifted V band is between the two observed bands. 3) Some systems have very uncertain host extinction or host galaxy contribu-

tion. 4) Some systems lack enough data to do polynomial fits to obtain light curves. e.g., for 2nd order, at least 3 data points are required. In practice, to obtain well defined light curves, more data points are needed. Below we provide a brief discussion for each system. The reasons for these systems being excluded from our analysis are summarized in Table 3.

**GRB 970228** At  $z = 0.695 \pm 0.002$  (Galama et al. 2000) I band data are collected. However, there are not enough data ( $< 3$ ) around the peak in the I band.

**GRB 990712** The V and I bands (Björnsson et al. 2001; Christensen et al. 2004; Sahu et al. 2000) have less than 3 data points after subtracting the afterglow brightness. In the R band, there are not enough data points to perform polynomial fitting.

**GRB 011121/SN 2001ke** At  $z = 0.36$  (Bloom et al. 2002) R and I band data (Bloom et al. 2002; Garnavich et al. 2003; Greiner et al. 2003; Küpcü Yoldaş et al. 2007) are collected. The host and the afterglow brightness are subtracted. Then there are not enough data around peak to do polynomial fitting in the I band. In addition, the host extinction is very uncertain.

**XRF 020903** After subtracting the afterglow brightness, there are not enough useful data points to do the polynomial fitting (Bersier et al. 2006; Soderberg et al. 2005).



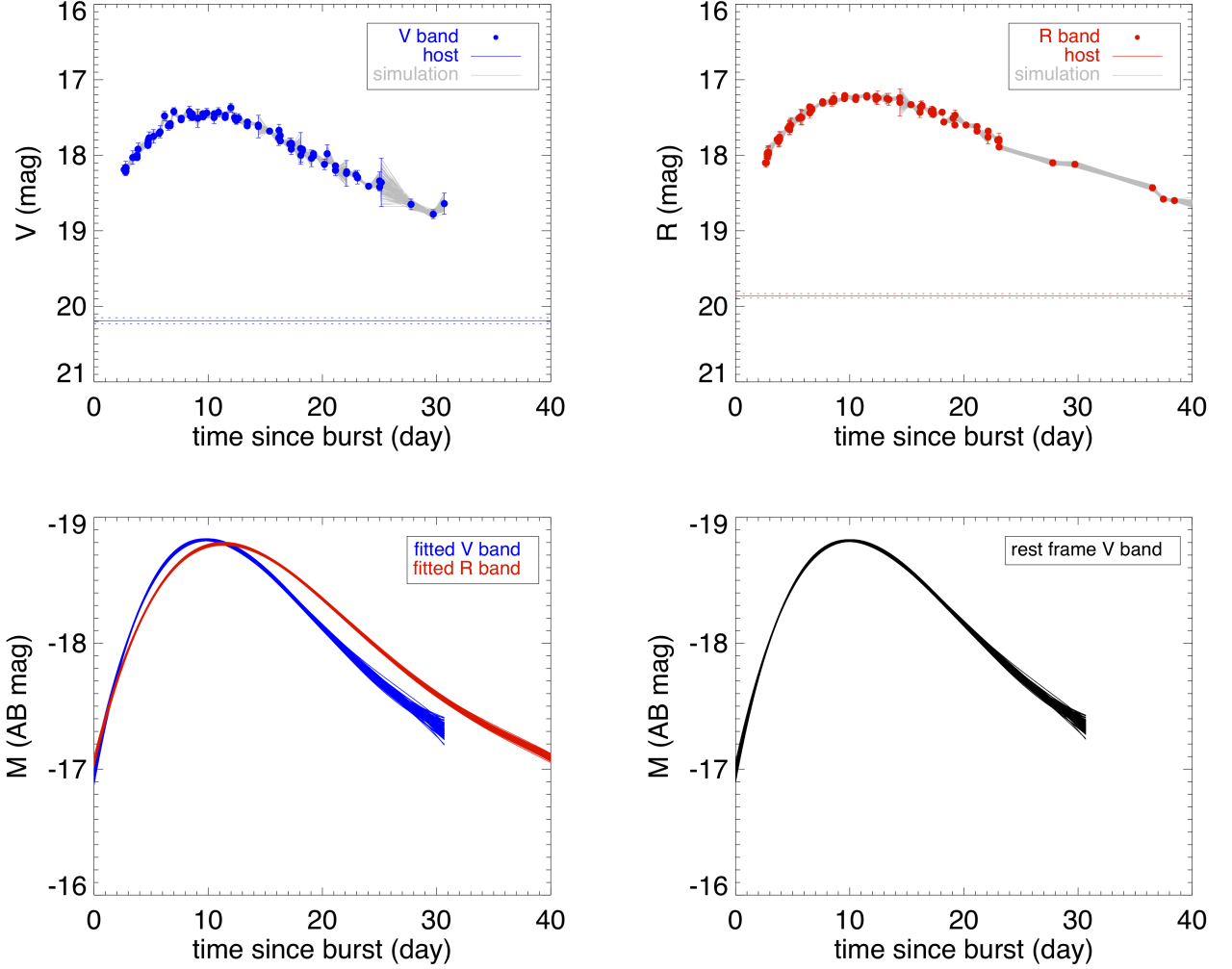


**Fig. 6.** XRF 060218 (SN 2006aj). The line styles are the same as in Figure 3.

**Table 3.** A list of unselected systems in class A, B, and C.

GRB/XRF/SN	reason(s)
970228	4
990712	1, 4
011121/2001ke	3, 4
020903	1
021211/2002lt	1
041106	2
080319B	1
081007/2008hw	3
091127	1
101219B/2012ma	4
120714B/2012eb	4

- 1: After subtracting the afterglow, there are too few data points left to obtain full light curves.
- 2: Lack of data in proper band(s) to do K-correction.
- 3: Uncertain host extinction or host galaxy contribution.
- 4: Lack of sufficient data around the peak to do polynomial fitting.

**GRB 021211/SN 2002lt** After subtracting the host and afterglow flux, there are too few data points left ( $< 3$ ) (Della Valle et al. 2003) to obtain light curves.

**GRB 041006** Only in the R band there are enough data (Stanek et al. 2005) to extract the light curve. But at a redshift of  $z = 0.716$ , the R band is too far from the rest frame V band.

**GRB 080319B** The redshift is  $z = 0.937$  and the data (Tanvir et al. 2010; Bloom et al. 2009) are in the R and I bands. The host contributions are  $R_{\text{host}} = 26.96 \pm 0.13$  mag and  $I_{\text{host}} = 26.17 \pm 0.15$  mag. The afterglow slope is fixed to  $\beta_2 = 2.33$  (Tanvir et al. 2010; Bloom et al. 2009). After subtracting the afterglow brightness there are not enough useful data points left to fit polynomial functions.

**GRB 081007/SN 2008hw** The redshift is  $z = 0.5295$  and the data are in the  $r'$  and  $i'$  bands (Jin et al. 2013). For the afterglow fitting, we fixed the slope to  $\beta_2 = 1.25$ , based on the X-ray observation (Jin et al. 2013). A multi-band K-correction is applied. But the host contribution is uncertain. If we assume it has host  $r_{\text{host}} = 25.0$  mag and  $i_{\text{host}} = 24.5$  mag, then the peak magnitude is  $M_{V,\text{peak}} = -18.85^{+0.91}_{-0.64}$  mag. However, a different estimate of the host galaxy brightness would lead to different peak magnitudes.

**GRB 091127** The redshift is  $z = 0.49$  and the data are collected from Troja et al. (2012); Vergani et al. (2011); Cobb et al. (2010). The  $i$  band data are selected. We subtract the host brightness with  $I_{\text{host}} = 22.54 \pm 0.10$  mag (Troja et al. 2012). The afterglow is fitted with broken power-law functions. But

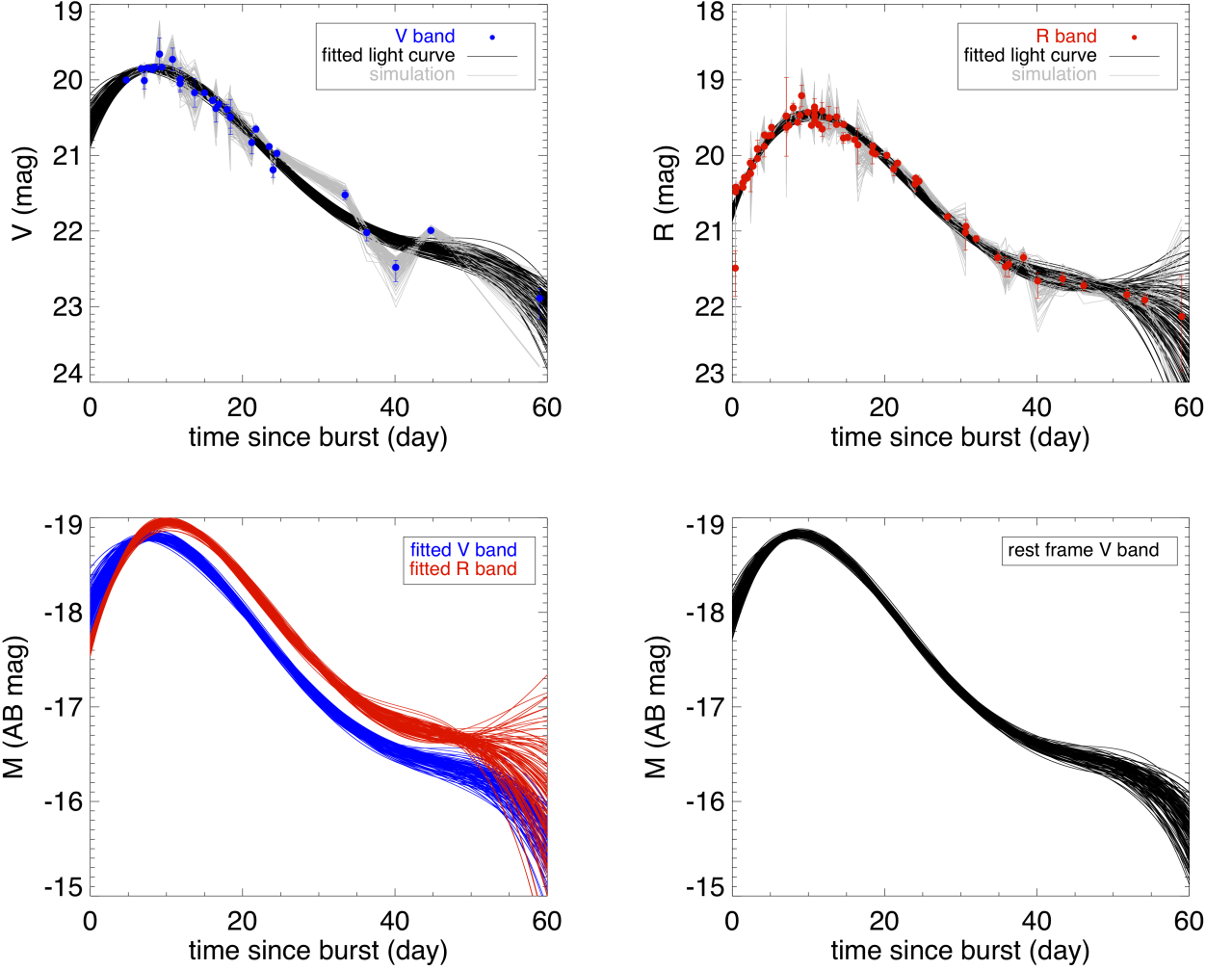


**Fig. 7.** XRF 100316D/SN 2010bh. The line styles are the same as in Figure 3.

after the afterglow fitting, there are not enough data to obtain light curves and measure the peak magnitude and the decline rate.

**GRB 101219B/SN 2010ma** With only two data points and an upper limit (Sparre et al. 2011), it is not possible to obtain the light curve.

**GRB 120714B/SN 2012eb** SN 2012eb was confirmed to be associated with GRB 120714B by Klose et al. (2012). But there are no published data for SN 2012eb yet.

#### 4. Properties of the light curves

The peak magnitudes, the decline rate in 15 days, the time of peak (see section 4.2.1) of the eight GRB-SNe are listed in Table 4. For SNe Ia, there is a relation between the intrinsic peak magnitude  $M_{V,\text{peak}}$  and decline rate  $\Delta m_{B,15}$  (Phillips 1993; Phillips et al. 1999). In addition,  $\Delta m_{V,15}$  is used in this paper to check if the light curves of SN 1998bw can be used as light curve templates and if there is a better way to do the rescaling other than using the  $s$  factor.

**Table 4.** The selected systems and relevant results with  $1\sigma$  uncertainties.

GRB/XRF/SN	$z$	$M_{V,\text{peak}}^a$ (mag)	$\Delta m_{V,15}$ (mag)	$t_{\text{peak}}$ (day)
980425/1998bw	0.0085	$-19.29^{+0.08}_{-0.08}$	$0.75^{+0.02}_{-0.02}$	$16.09^{+0.17}_{-0.18}$
030329/2003dh	0.1685	$-19.39^{+0.14}_{-0.12}$	$0.90^{+0.50}_{-0.50}$	$10.74^{+2.37}_{-0.85}$
031203/2003lw	0.1055	$-19.90^{+0.16}_{-0.16}$	$0.64^{+0.10}_{-0.10}$	$19.94^{+1.37}_{-1.48}$
050525A/2005nc	0.606	$-18.59^{+0.31}_{-0.25}$	$1.17^{+0.69}_{-0.88}$	$11.08^{+2.26}_{-3.37}$
060218/2006aj	0.03342	$-18.85^{+0.08}_{-0.08}$	$1.08^{+0.06}_{-0.06}$	$9.96^{+1.18}_{-0.18}$
090618	0.54	$-19.34^{+0.13}_{-0.13}$	$0.65^{+0.15}_{-0.17}$	$17.54^{+1.51}_{-1.64}$
100316D/2010bh	0.059	$-18.89^{+0.10}_{-0.10}$	$1.10^{+0.05}_{-0.05}$	$8.76^{+0.31}_{-0.37}$
120422A/2012bz	0.283	$-19.50^{+0.03}_{-0.03}$	$0.73^{+0.06}_{-0.06}$	$14.20^{+0.34}_{-0.34}$

$a$ : The uncertainties in  $M_{V,\text{peak}}$  quadratically come from the polynomial fits, the 0.02 mag in K correction, the distance modulus uncertainties and the uncertainties in the host extinction.

##### 4.1. Luminosity-decline rate relation

###### 4.1.1. $M_{V,\text{peak}} = f(\Delta m_{V,15})$

Though the physical progenitors and explosion mechanisms for SNe Ia and GRB-SNe are different (Hillebrandt & Niemeyer

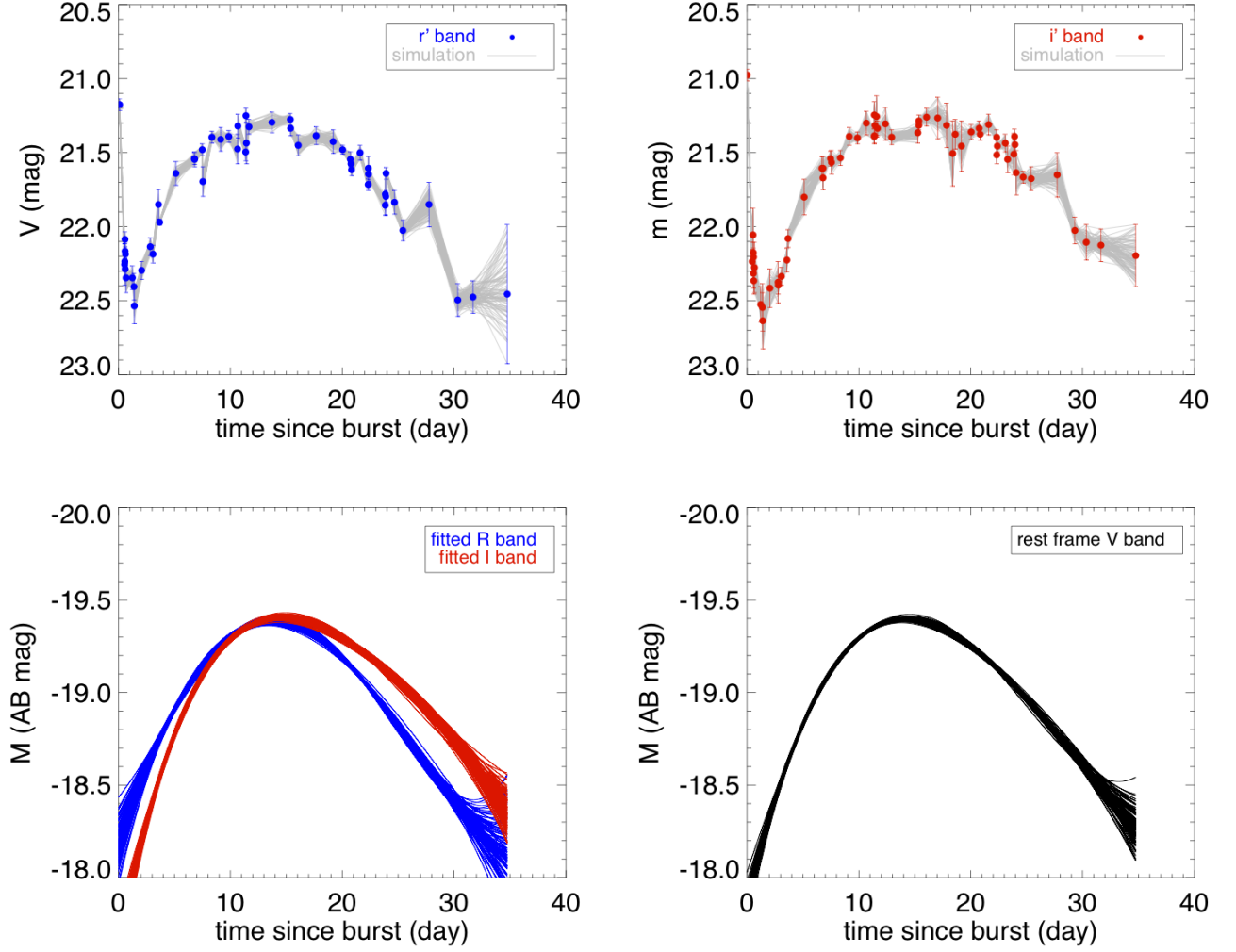


**Fig. 8.** GRB 120422A/SN 2012bz. The line styles are the same as in Figure 3.

2000; Smartt 2009), their light curves show similar luminosity-decline rate relations. The peak magnitude and the decline rate are resimulated 10 000 times each. The widths of the distribution of the resimulated data are  $1\sigma$ . We linearly fit each set of the resimulated data and get two distributions of the fitting parameters. The median values and  $\pm 1\sigma$  values on two sides of the median values in these two distributions are treated as the best fitting parameters and the  $\pm 1\sigma$  uncertainties. The luminosity-decline rate relation for GRB-SNe is

$$M_{V,\text{peak}} = 1.59^{+0.28}_{-0.24} \Delta m_{V,15} - 20.61^{+0.19}_{-0.22}, \quad (4)$$

with  $\chi^2 = 5.2$  (6 dof). Figure 9 shows the luminosity-decline rate relation with  $\alpha = 5, 10,$  and  $15$  days. Systems GRB 031203/SN 2003lw and GRB 100316D/SN 2010bh have uncertain extinction, so they are plotted as open symbols. Unless mentioned otherwise, these two systems are discerned in the same way in the following figures. Some systems lack data to constrain light curves at large times, i.e.,  $\alpha > 15$  days, so we cannot get  $\Delta m_{V,>15}$  for these systems. This relation shows that (1) the peak magnitudes span a small range; (2) the trend of the relation is the same as for SNe Ia, i.e., brighter systems decline slower. Though there could be significant selection effects, in that we only have good data for bright systems.

#### 4.1.2. Correlation coefficients and significance

With the standard Monte Carlo method, the correlation coefficients: Pearson's, Kendal's  $\tau$  and Spearman's rank, are calculated to statistically measure the strength of the correlation between the peak magnitudes and the decline rates. As in section 4.1.1, the peak magnitude  $M_{V,\text{peak}}$  and the decline rate  $\Delta m_{V,15}$  are resimulated 10 000 times each, where  $1\sigma$  are the widths of the distribution of the resimulated data. For each set of resimulated data, we calculate three correlation coefficients.

Pearson's correlation coefficient (Pearson's  $r$ ) measures the linear correlation between two variables. The result  $r \in [-1, 1]$ , where 1 (−1) is total positive (negative) correlation, and 0 is no correlation. When  $|r| > 0.7$  (or 0.8 by different suggestion), the correlation is described as 'very strong'. If bin size is set to 0.01 (same in the following),  $r = 0.905$  has the highest frequency and this shows the correlation is significant at 0.01 level. This means we expect to get the result occurring by chance once every 100 times. The result indicates a significant correlation between  $M_{V,\text{peak}}$  and  $\Delta m_{V,15}$ . There are [93%, 87%, 63%, 9%] of Pearson's correlation coefficients lie at [0.1, 0.05, 0.01, 0.001] significance levels.

Kendal's rank correlation coefficient (Kendal's  $\tau$ ) measures the strength of the monotonic relationship between variables.

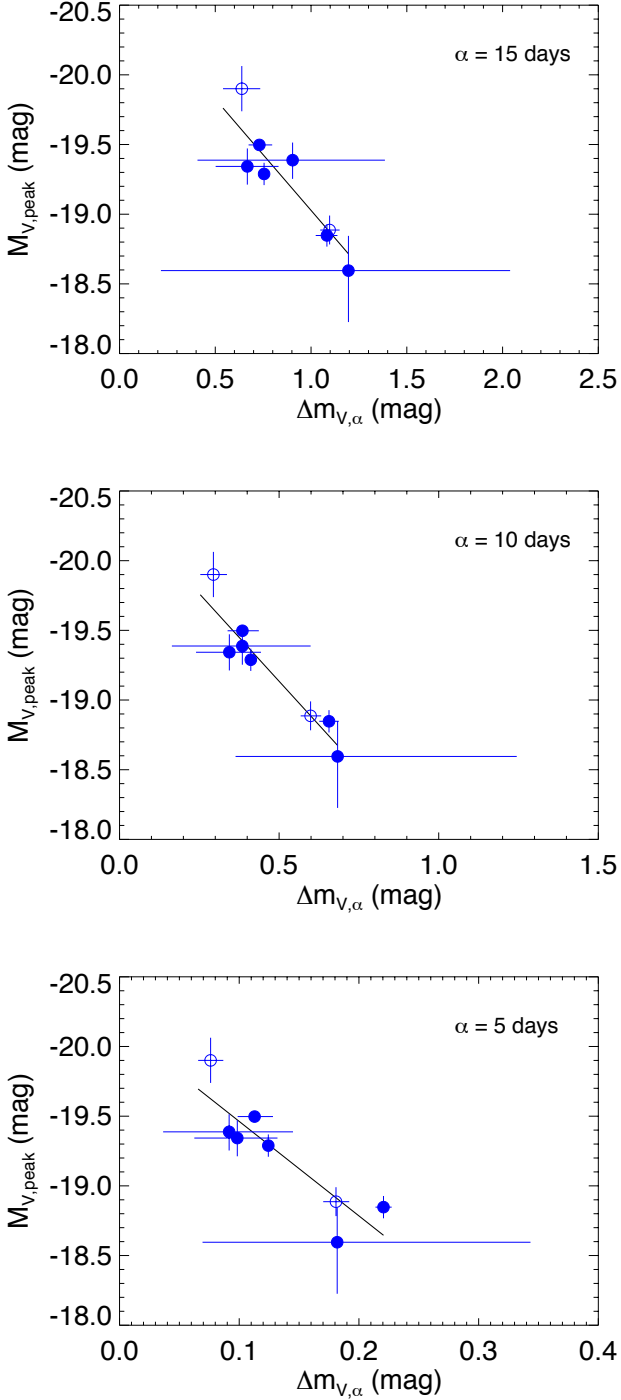


**Fig. 9.** The peak-luminosity and decline rate relation for GRB-SNe with the decline times of 5, 10 and 15 days. Systems GRB 031203/SN 2003lw and GRB 100316D/SN 2010bh have uncertain extinction, and they are plotted as open symbols. The best linear fits to the relations are in black.

The result  $\tau \in [-1, 1]$ , where  $1/-1$  imply the perfect agreement/disagreement between two rankings and 0 means the ranking is totally independent. In this paper,  $\tau = 0.715$  has the highest frequency and the corresponding significance level is 0.01. There are [91%, 79%, 43%, 0.3%] of Kendall's rank correlation coefficients lie at [0.1, 0.05, 0.01, 0.001] significance levels.

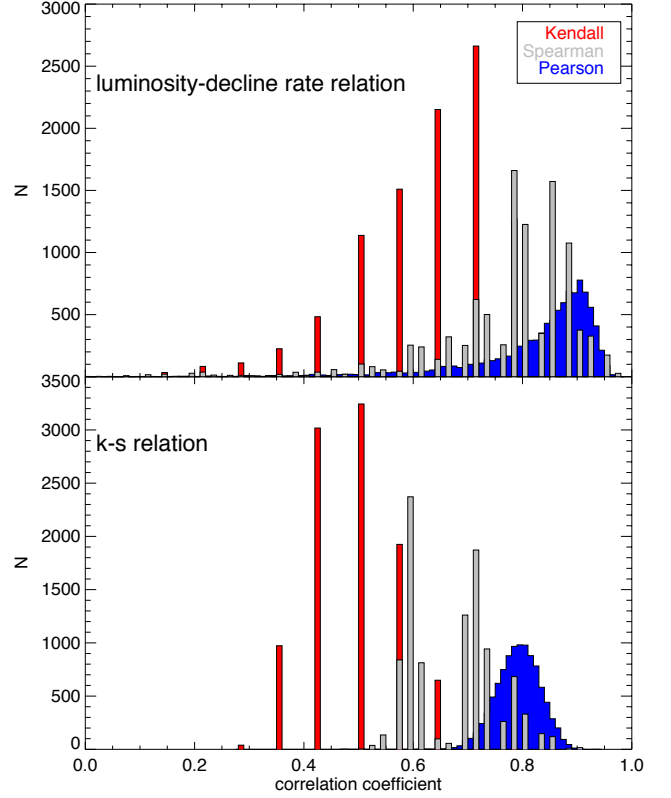


**Fig. 10.** Kendal's  $\tau$ , Spearman's rank, and Pearson's correlation coefficients of the luminosity-decline rate relation in the upper panel and the  $k - s$  relation (section 4.2.2) in the bottom panel. Bin size is 0.01.  $M_{V,\text{peak}}$ ,  $\Delta m_{V,15}$ , the  $k$  factor and the  $s$  factor are resimulated 10 000 times with the standard Monte Carlo method.

Spearman's rank correlation coefficient (Spearman's  $\rho$ ) tests the dependence between two variables. The result  $\rho \in [-1, 1]$ , where  $-1$  or  $+1$  appears when the relation of the variables can be perfectly described with a monotonic function. When  $|\rho| \geq 0.6$ , the correlation is described as 'strong'. In this paper,  $\rho = 0.785$  has the highest frequency and the corresponding significance level is 0.025. There are [95%, 87%, 30%, 2%] of Spearman's rank correlation coefficients lie at [0.1, 0.05, 0.01, 0.001] significance levels.

**Table 5.** The most frequent values and the percentage of the correlation coefficients at different significance levels. Here we set the bin size equal to 0.01.

coefficient	significance level <sup>a</sup>				most frequent value
	0.1	0.05	0.01	0.001	
luminosity-decline rate relation					
Pearson's	93%	87%	63%	9%	0.905
Kendal's $\tau$	91%	79%	43%	0.3%	0.715
Spearman's rank	95%	87%	30%	2%	0.785
$k - s$ relation					
Pearson's	99%	97%	14%	~ 0%	0.795
Kendal's $\tau$	60%	27%	1.5%	~ 0%	0.505
Spearman's rank	99%	57%	3%	~ 0%	0.595

<sup>a</sup>: The probability of accidentally getting the result, e.g., 0.05 represents the result happens by chance once every 20 times.

The distributions of the correlation coefficients of the luminosity-decline rate relation are plotted in the upper panel in Figure 10. The most frequencies and the percentage of the correlation coefficients at different significance levels are listed in Table 5. The statistical correlation coefficients show that the luminosity and the decline rate of GRB-SNe are significantly correlated.

## 4.2. Time since burst

### 4.2.1. Peak time

The peak time  $t_{\text{peak}}$  is defined as the time when the light curve of a GRB-SN reaches its peak brightness relative to the time of the GRB in the rest frame. The peak times for the eight systems are listed in Table 4. With the same procedure as in section 4.1.1, the best fit to the relation between  $\log t_{\text{peak}}$  and  $M_{V,\text{peak}}$  is

$$M_{V,\text{peak}} = -2.52^{+0.16}_{-0.15} \log t_{\text{peak}} - 16.41^{+0.16}_{-0.18}. \quad (5)$$

When combining the two parameters  $\log t_{\text{peak}}$  and  $\Delta m_{V,15}$ , regression fit to  $M_{V,\text{peak}}$  can be expressed as

$$M_{V,\text{peak}} = 1.46^{+0.73}_{-0.88} \Delta m_{V,15} - 0.29^{+1.01}_{-1.41} \log t_{\text{peak}} - 20.19^{+2.34}_{-1.74}. \quad (6)$$

The relation between  $\log t_{\text{peak}}$  and  $\Delta m_{V,15}$  can be expressed as

$$\log t_{\text{peak}} = -0.51^{+0.13}_{-0.11} \Delta m_{V,15} + 1.56^{+0.09}_{-0.10}. \quad (7)$$

Figure 11 shows the relations between  $\log t_{\text{peak}}$ ,  $\Delta m_{V,15}$  and  $M_{V,\text{peak}}$ . The upper panel shows that there is a dependency between the peak time  $t_{\text{peak}}$  and the peak magnitude  $M_{V,\text{peak}}$ . There is a trend that a GRB-SN with smaller peak time has fainter peak luminosity, i.e.,  $M_{V,\text{peak}}$  decreases as  $t_{\text{peak}}$  increases. In general, brighter GRB-SNe evolve more slowly. Compared to Figure 9,  $t_{\text{peak}}$  is less strongly correlated with  $M_{V,\text{peak}}$  than  $\Delta m_{V,15}$ . The middle panel shows a multiple linear regression fit to  $M_{V,\text{peak}}$  with  $\log t_{\text{peak}}$  and  $\Delta m_{V,15}$ . The bottom panel of Figure 11 shows a ‘fundamental plane’ of GRB-SNe with peak time  $t_{\text{peak}}$  and decline rate  $\Delta m_{V,15}$ . Constant absolute peak magnitudes are also indicated by dotted lines.

### 4.2.2. $k - s$ relation

Besides the peak magnitude  $M_{V,\text{peak}}$  and the decline rate  $\Delta m_{V,a}$ , another way to describe the light curve is through the luminosity factor  $k$  and the stretch factor  $s$ . These two factors stand for the relative peak ( $k$ ) and width ( $s$ ) of the light curves compared to SN 1998bw (Cano et al. 2011a):

$$f(t) = k \times f^{98\text{bw}}(t/s), \quad (8)$$

Here  $f(t)$  is the flux of a SN, and  $f^{98\text{bw}}(t)$  is the flux of SN 1998bw. The factor  $s$  equals to  $t_{\text{peak}}/t_{\text{peak}}^{98\text{bw}}$ , with  $t_{\text{peak}}^{98\text{bw}}$  representing the peak time of SN 1998bw. With the same procedure as in section 4.1.1, the  $s$  and  $k$  factors are correlated as

$$k = 1.25^{+0.12}_{-0.12} \cdot s - 0.05^{+0.09}_{-0.09}, \quad (9)$$

with  $\chi^2 = 8.2$  (6 dof). This relation is named as  $k - s$  relation. Figure 12 shows the correlations between  $s$ ,  $k$ , the decline rate  $\Delta m_{V,15}$  and the peak magnitude  $M_{V,\text{peak}}$ .

With the procedure discussed in section 4.1.2, the distributions of the correlation coefficients of the  $k - s$  relation are plotted in the lower panel in Figure 10. The most frequencies and the percentage of the correlation coefficients at different significance

levels are listed in Table 5. Comparing the results in Figures 9, 11, 12 and Table 5, we conclude that 1) the correlation between  $\Delta m_{V,15}$  and  $M_{V,\text{peak}}$  is stronger than the one between factors  $k$  and  $s$ . 2)  $\Delta m_{V,15}$  is stronger correlated with  $M_{V,\text{peak}}$  than  $t_{\text{peak}}$  and the  $s$  factor.

## 4.3. Rescaling of light curves

To test if the light curve of SN 1998bw can be used as a template for other GRB-SN light curves, we rescale the light curves in three ways. In all cases,  $M_{V,\text{peak}}$  has been normalized relative to SN 1998bw.

**$\Delta m_{15}$  rescaling** The light curves are rescaled around  $t_{\text{peak}}$ . The time of the light curve is calculated as  $t' = (t - t_{\text{peak}}) \times \Delta m_{V,15} / \Delta m_{15}^{98\text{bw}} + t_{\text{peak}}^{98\text{bw}}$ , with  $\Delta m_{15}^{98\text{bw}}$  and  $t_{\text{peak}}^{98\text{bw}}$  representing the decline rate and the peak time of SN 1998bw.

**$s$  factor rescaling** The light curves are rescaled as  $t' = t/s$ , with  $s$  being the stretch factor.

**$\log(t_{\text{peak}})$  rescaling** The light curves are rescaled around  $t_{\text{peak}}$ . The time is calculated as  $t' = (t - t_{\text{peak}}) \times \log(t_{\text{peak}}^{98\text{bw}}) / \log(t_{\text{peak}}) + t_{\text{peak}}^{98\text{bw}}$ .

A collection of rescaled light curves for the selected systems are shown in Figure 13. The fitting curves are the rest frame V band light curves obtained in section 3. The data points are for illustration and are from the bands closest to the rest frame V band. The figure shows that a rescaled SN 1998bw light curve is a reasonable template for other GRB-SN light curve.  $\Delta m_{15}$  rescaling appears superior to the other approaches. If values of  $\Delta m_{15}$  are not available,  $\log(t_{\text{peak}})$  rescaling is an alternative to the commonly used  $s$  factor rescaling.

## 4.4. Discussion

We compare the values of the peak magnitudes to other studies (Malesani et al. 2004; Cano et al. 2011a,b; Cano 2013; Schulze et al. 2014). The result is shown in Figure 14. There are three obvious outliers: GRB 090618, SN 2010bh and SN 2012bz. These systems are estimated to have fainter peak magnitudes in this paper. It is difficult to trace the exact causes of the differences in the peak magnitudes. We follow the procedure from the literature, and compare it to our results.

There is no independent third-part study for the peak magnitude of GRB 090618. The peak magnitude is estimated to be  $M_{V,\text{peak}} = -19.34^{+0.13}_{-0.13} (-19.75^{+0.14}_{-0.14})$  mag from this paper (Cano et al. 2011b). The reasons cause the difference are: 1) With different cosmological parameters, the distance modulus is different. We adopt distance modulus  $\mu = 42.53$  with the cosmological parameters  $\{\Omega_M, \Omega_\Lambda, h\} = \{0.315, 0.685, 0.673\}$ , while  $\mu = 42.45$  from Cano et al. (2011b). 2) The subtraction of the afterglow may be another reason for the discrepancy. This may cause  $\sim 0.15$  mag difference around the peak. The observed peak magnitude is  $i = 22.33$  mag. After the host and the afterglow subtraction with  $i_{\text{host}} = 23.22 \pm 0.06$  mag, the peak magnitude becomes  $i = 22.96$  mag and  $i = 23.13$  mag, respectively. From Cano et al. (2011b) the apparent peak magnitude is  $i = 23.00$  mag. 3) The polynomial fitting may bring  $\sim 0.08$  mag difference. The fitted (observed) apparent peak magnitude is  $i = 23.21$  (23.13) mag. Figure 5 shows the observed data. Around peak, the data are noisy. At  $t = 16.69$  and  $17.60$  days, the magnitudes are  $\sim 0.2$  and  $0.04$  mag fainter than the one at  $t = 14.79$ . Instead of using a single datum, in this paper, polynomial functions are fitted, especially around the peak. 4) The Galactic extinction is different. In

this paper, we use  $R_V = 3.1$  as well as the re-calibration results of DIRBE/IRAS dust map from Schlafly & Finkbeiner (2011). This may bring  $\sim 0.15$  mag difference.

For XRF 100316D/SN 2010bh, the peak magnitude is constrained to be  $M_{V,\text{peak}} = -18.89^{+0.10}_{-0.10} / -18.62 \pm 0.08$  mag in this paper/Cano et al. (2011a). This is a system with uncertain host extinction and peak magnitude. The reasons are: 1) The values in Cano et al. (2011a) are inconsistent. In Table 2 (Cano et al. 2011a), the apparent peak magnitude in the V band is 19.47 mag after the Galactic extinction correction. So if  $R_V = 3.1$  and K correction  $\Delta k = 0.09$  are used in his calculation, the peak magnitude should be  $M_{V,\text{peak}} = m_V - \mu - A_{V,\text{host}} - \Delta K = 19.47 - 37.08 - 0.18 \cdot 3.1 - 0.09 = -18.26$  mag instead of  $-19.62$  mag, which is listed in Table 4 (Cano et al. 2011a). The photometric data from Cano et al. (2011a) is consistent with the result from Bufano et al. (2012), so we guess the foreground extinction is subtracted twice in the calculation, which is consistent with the statement of the captions of Table 2 and 4. The result also shows that a larger host extinction is expected, otherwise the spectrum is very red (as stated in section 3.7). 2) The host extinction estimated in the literature are different. We adopt a large extinction with  $E(B - V)_{\text{host}} = 0.39 \pm 0.03$  mag from Olivares E. et al. (2012). The value of  $E(B - V)_{\text{host}} = 0.18 \pm 0.08$  mag is estimated in Cano et al. (2011a). This may cause  $\sim 0.64$  mag difference. 3) The distance moduli are different. In this paper,  $\mu = 37.20$  while Cano et al. (2011a) adopts  $\mu = 37.08$ . This causes about 0.12 mag difference. 4) The K correction in (Cano et al. 2011a) may bring about 0.09 mag difference.

For GRB 120422A/SN 2012bz, the peak magnitude is estimated to be  $M_{V,\text{peak}} = -19.50^{+0.03}_{-0.03} / -19.7$  mag in this paper/Schulze et al. (2014), while using the same cosmological parameters (Planck Collaboration et al. 2013), Leloudas (2014) estimates the peak magnitude to be  $-19.63$  mag. The reasons of the discrepancies may be as follows: 1) The Galactic extinction may be corrected twice in calculating the absolute peak magnitude (Schulze et al. 2014; Leloudas 2014). So the magnitude should be about 0.09 mag fainter. 2) In addition,  $R_V$  instead of  $R_I$  may be multiplied in calculating the Galactic extinction. This may in further bring about  $\sim 0.05$  mag difference. 3) As discussed above, the noisy data around the peak may bring about 0.03 mag difference.

Figure 15 shows the comparison of peak time in this paper (in Table 4) and the stretch factor  $s$  from Cano (2013). There is no information on  $s_V$  for systems SN 2003dh, SN 2003lw, GRB 050525A and GRB 090618, so  $s_R$  is used instead.

## 5. Conclusions

We developed a method for obtaining the light curves in the rest frame V band from the observational data. A standard Monte Carlo method was used for error estimation. Afterglow and host brightness were subtracted. We used the DIRBE/IRAS dust map and the correction coefficients to correct the foreground extinction. The host extinction was corrected. We used a multi-band K-correction to correct the light curves from the observed bands into the rest frame V band. Alternatively, SN 1998bw peak SED and decline rate templates were used when a multi-band K-correction is not feasible. Polynomial functions were fitted to obtain the light curves.

Based on this method we obtained the peak magnitudes and the decline rates for eight GRB-SN systems in classes A, B, and C. We discovered a relation between the peak magnitude and the decline rate. This luminosity-decline rate relation was tested with the decline day  $\alpha$  at 5, 10 and 15 days. The strength of the

relationship between the peak magnitude and the decline rate was statistically measured by three correlation coefficients and the significance levels were discussed. There is a dependency between the peak magnitude and the peak time. The larger the peak time, the brighter the SN is. We found that the light curve of SN 1998bw can be used as a representative template. In addition, rescaling around the peak time with  $\Delta m_{V,15}$  is better than rescaling with peak time  $\log t_{\text{peak}}$  or stretch factor  $s$ . We also compared the peak magnitudes and the decline rates constrained from this work to the results from other studies.

SNe Ia and GRB-SNe have completely different progenitors. Nevertheless, the light curves have similar peak magnitudes and decline rates. This phenomenon may potentially help us shed light on progenitor models of GRBs. As SNe Ia are widely used as standard candles to measure cosmological distances, it is possible that GRB-SNe may also turn out to be useful high-redshift standard candles. In particular, the prospects of studying dark energy through  $w(z)$  with GRB-SNe using the James Webb Space Telescope (JWST) is intriguing.

*Acknowledgements.* We thank Enrico Ramirez-Ruiz, Tamara Davis Giorgos Leloudas and Radek Wojtak for their many helpful discussions and comments on the paper. We thank Teddy Frederiksen, Darach Watson, Daniele Malesani and Dong Xu for discussions on GRB and SNe. The Dark Cosmology Centre is funded by the Danish National Research Foundation.

## References

- Bersier, D., Fruchter, A. S., Strolger, L.-G., et al. 2006, *ApJ*, 643, 284  
 Björnsson, G., Hjorth, J., Jakobsson, P., Christensen, L., & Holland, S. 2001, *ApJ*, 552, L121  
 Bloom, J. S., Kulkarni, S. R., Djorgovski, S. G., et al. 1999, *Nature*, 401, 453  
 Bloom, J. S., Kulkarni, S. R., Price, P. A., et al. 2002, *ApJ*, 572, L45  
 Bloom, J. S., Perley, D. A., Li, W., et al. 2009, *ApJ*, 691, 723  
 Blustin, A. J., Band, D., Barthelmy, S., et al. 2006, *ApJ*, 637, 901  
 Bufano, F., Pian, E., Sollerman, J., et al. 2012, *ApJ*, 753, 67  
 Campana, S., Mangano, V., Blustin, A. J., et al. 2006, *Nature*, 442, 1008  
 Cano, Z. 2013, *MNRAS*, 434, 1098  
 Cano, Z., Bersier, D., Guidorzi, C., et al. 2011a, *ApJ*, 740, 41  
 Cano, Z., Bersier, D., Guidorzi, C., et al. 2011b, *MNRAS*, 413, 669  
 Cardelli, J. A., Clayton, G. C., & Mathis, J. S. 1989, *ApJ*, 345, 245  
 Christensen, L., Hjorth, J., Gorosabel, J., et al. 2004, *A&A*, 413, 121  
 Clocchiatti, A., Suntzeff, N. B., Covarrubias, R., & Candia, P. 2011, *AJ*, 141, 163  
 Cobb, B. E., Bloom, J. S., Perley, D. A., et al. 2010, *ApJ*, 718, L150  
 Davis, T. 2013, private communication  
 Della Valle, M., Malesani, D., Benetti, S., et al. 2003, *A&A*, 406, L33  
 Della Valle, M., Malesani, D., Bloom, J. S., et al. 2006, *ApJ*, 642, L103  
 Ferrero, P., Kann, D. A., Zeh, A., et al. 2006, *A&A*, 457, 857  
 Fixsen, D. J., Cheng, E. S., Gales, J. M., et al. 1996, *ApJ*, 473, 576  
 Fynbo, J. P. U., Watson, D., Thöne, C. C., et al. 2006, *Nature*, 444, 1047  
 Gal-Yam, A., Fox, D. B., Price, P. A., et al. 2006, *Nature*, 444, 1053  
 Galama, T. J., Tanvir, N., Vreeswijk, P. M., et al. 2000, *ApJ*, 536, 185  
 Galama, T. J., Vreeswijk, P. M., van Paradijs, J., et al. 1998, *Nature*, 395, 670  
 Garnavich, P. M., Stanek, K. Z., Wyrzykowski, L., et al. 2003, *ApJ*, 582, 924  
 Gehrels, N., Norris, J. P., Barthelmy, S. D., et al. 2006, *Nature*, 444, 1044  
 Greiner, J., Klose, S., Salvato, M., et al. 2003, *ApJ*, 599, 1223  
 Guenther, E. W., Klose, S., Vreeswijk, P., Pian, E., & Greiner, J. 2006, GRB Coordinates Network, 4863, 1  
 Heise, J., Zand, J. I., Kippen, R. M., & Woods, P. M. 2001, in *Gamma-ray Bursts in the Afterglow Era*, ed. E. Costa, F. Frontera, & J. Hjorth, 16  
 Hillebrandt, W. & Niemeyer, J. C. 2000, *ARA&A*, 38, 191  
 Hjorth, J. 2013, *Royal Society of London Philosophical Transactions Series A*, 371, 20275  
 Hjorth, J. & Bloom, J. S. 2012, *The Gamma-Ray Burst - Supernova Connection*, 169–190  
 Hjorth, J., Sollerman, J., Møller, P., et al. 2003, *Nature*, 423, 847  
 Hogg, D. W., Baldry, I. K., Blanton, M. R., & Eisenstein, D. J. 2002, *ArXiv Astrophysics e-prints*  
 Iwamoto, K., Mazzali, P. A., Nomoto, K., et al. 1998, *Nature*, 395, 672  
 Jin, Z.-P., Covino, S., Della Valle, M., et al. 2013, *ApJ*, 774, 114  
 Klebesadel, R. W., Strong, I. B., & Olson, R. A. 1973, *ApJ*, 182, L85  
 Klose, S., Greiner, J., Fynbo, J., et al. 2012, *Central Bureau Electronic Telegrams*, 3200, 1

Kouveliotou, C., Meegan, C. A., Fishman, G. J., et al. 1993, *ApJ*, 413, L101  
 Kulkarni, S. R., Frail, D. A., Wieringa, M. H., et al. 1998, *Nature*, 395, 663  
 Küpcü Yoldaş, A., Salvato, M., Greiner, J., et al. 2007, *A&A*, 463, 893  
 Leloudas, G. 2014, private communication  
 Levan, A. J., Tanvir, N. R., Fruchter, A. S., et al. 2013, *ArXiv e-prints*  
 Li, X., Hjorth, J., & Wojtak, R. 2014  
 MacFadyen, A. I. & Woosley, S. E. 1999, *ApJ*, 524, 262  
 MacFadyen, A. I., Woosley, S. E., & Heger, A. 2001, *ApJ*, 550, 410  
 Malesani, D. 2013, private communication  
 Malesani, D., Tagliaferri, G., Chincarini, G., et al. 2004, *ApJ*, 609, L5  
 Matheson, T., Garnavich, P. M., Stanek, K. Z., et al. 2003, *ApJ*, 599, 394  
 Mazzali, P. A., Deng, J., Pian, E., et al. 2006, *ApJ*, 645, 1323  
 McBreen, S., Foley, S., Watson, D., et al. 2008, *ApJ*, 677, L85  
 Melandri, A., Pian, E., Ferrero, P., et al. 2012, *A&A*, 547, A82  
 Metzger, M. R., Djorgovski, S. G., Kulkarni, S. R., et al. 1997, *Nature*, 387, 878  
 Munari, U. & Zwitter, T. 1997, *A&A*, 318, 269  
 Ofek, E. O., Cenko, S. B., Gal-Yam, A., et al. 2007, *ApJ*, 662, 1129  
 Olivares E., F., Greiner, J., Schady, P., et al. 2012, *A&A*, 539, A76  
 Pei, Y. C. 1992, *ApJ*, 395, 130  
 Phillips, M. M. 1993, *ApJ*, 413, L105  
 Phillips, M. M., Lira, P., Suntzeff, N. B., et al. 1999, *AJ*, 118, 1766  
 Planck Collaboration, Ade, P. A. R., Aghanim, N., et al. 2013, *ArXiv e-prints*  
 Poznanski, D., Prochaska, J. X., & Bloom, J. S. 2012, *MNRAS*, 426, 1465  
 Prochaska, J. X., Bloom, J. S., Chen, H.-W., et al. 2004, *ApJ*, 611, 200  
 Richardson, D. 2009, *AJ*, 137, 347  
 Richardson, D., Branch, D., & Baron, E. 2006, *AJ*, 131, 2233  
 Riess, A. G., Filippenko, A. V., Challis, P., et al. 1998, *AJ*, 116, 1009  
 Sahu, K. C., Vreeswijk, P., Bakos, G., et al. 2000, *ApJ*, 540, 74  
 Schlafly, E. F. & Finkbeiner, D. P. 2011, *ApJ*, 737, 103  
 Schlegel, D. J., Finkbeiner, D. P., & Davis, M. 1998, *ApJ*, 500, 525  
 Schulze, S., Malesani, D., Cucchiara, A., et al. 2014, *ArXiv e-prints*  
 Smartt, S. J. 2009, *ARA&A*, 47, 63  
 Soderberg, A. M., Kulkarni, S. R., Fox, D. B., et al. 2005, *ApJ*, 627, 877  
 Sollerman, J., Holland, S. T., Challis, P., et al. 2002, *A&A*, 386, 944  
 Sollerman, J., Jaunsen, A. O., Fynbo, J. P. U., et al. 2006, *A&A*, 454, 503  
 Sparre, M., Sollerman, J., Fynbo, J. P. U., et al. 2011, *ApJ*, 735, L24  
 Stanek, K. Z., Garnavich, P. M., Nutzman, P. A., et al. 2005, *ApJ*, 626, L5  
 Stanek, K. Z., Matheson, T., Garnavich, P. M., et al. 2003, *ApJ*, 591, L17  
 Tanvir, N. R., Rol, E., Levan, A. J., et al. 2010, *ApJ*, 725, 625  
 Troja, E., Sakamoto, T., Guidorzi, C., et al. 2012, *ApJ*, 761, 50  
 Šimon, V., Pizzichini, G., & Hudec, R. 2010, *A&A*, 523, A56  
 van Dokkum, P. G. & Franx, M. 1996, *MNRAS*, 281, 985  
 van Paradijs, J., Groot, P. J., Galama, T., et al. 1997, *Nature*, 386, 686  
 Vergani, S. D., Flores, H., Covino, S., et al. 2011, *A&A*, 535, A127  
 Woosley, S. E. & Bloom, J. S. 2006, *ARA&A*, 44, 507  
 Woosley, S. E., Eastman, R. G., & Schmidt, B. P. 1999, *ApJ*, 516, 788  
 Xu, D., de Ugarte Postigo, A., Leloudas, G., et al. 2013, *ApJ*, 776, 98  
 Zeh, A., Klose, S., & Hartmann, D. H. 2004, *ApJ*, 609, 952

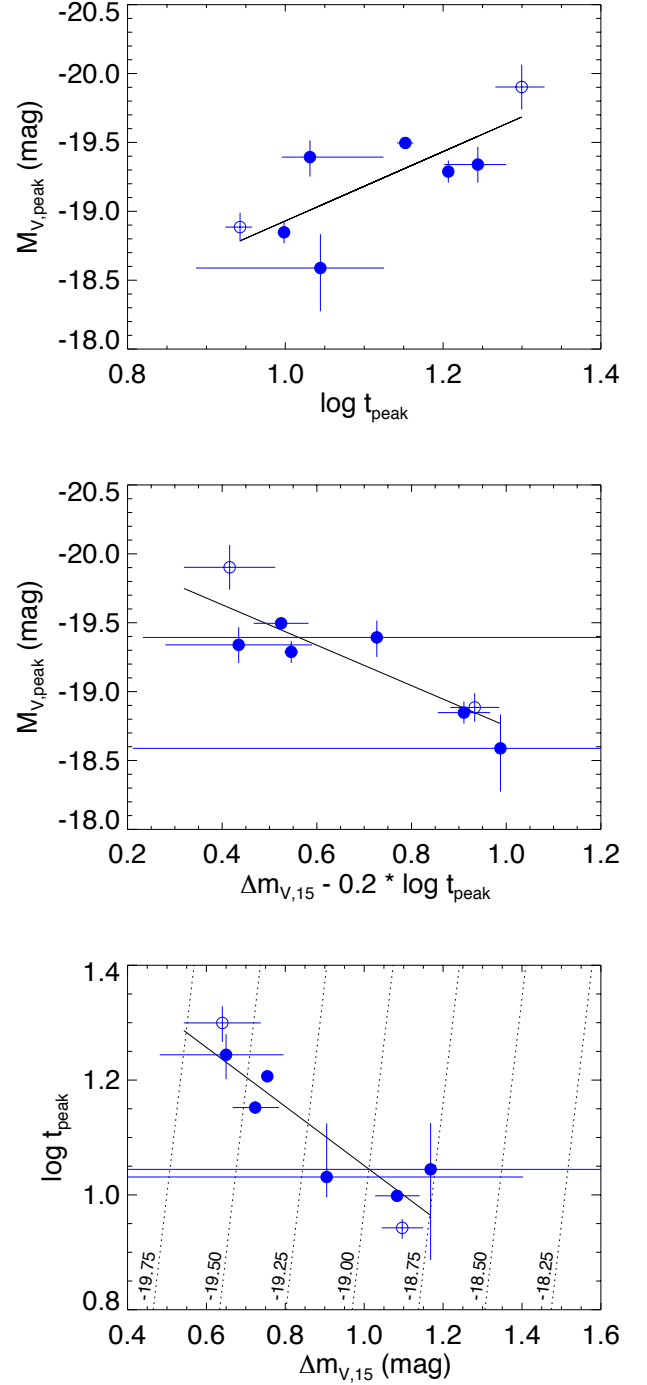


**Fig. 11.** The relations between logarithmic peak time  $\log t_{\text{peak}}$ , peak magnitude  $M_{V,\text{peak}}$  and decline rate  $\Delta m_{V,15}$ . The upper panel shows  $\log t_{\text{peak}}$  as a function of  $M_{V,\text{peak}}$ . The middle panel shows the multiple linear relation between  $\Delta m_{V,15}$ ,  $\log t_{\text{peak}}$  and  $M_{V,\text{peak}}$ . The bottom panel displays a ‘fundamental plane’ like relation for GRB-SNe through  $t_{\text{peak}}$  and  $\Delta m_{V,15}$ . The straight lines in blue are the best linear fitting functions (Eqs. 5, 7 and 6). The dotted lines indicate loci of equal absolute peak magnitudes. The best linear fits are plotted in black.

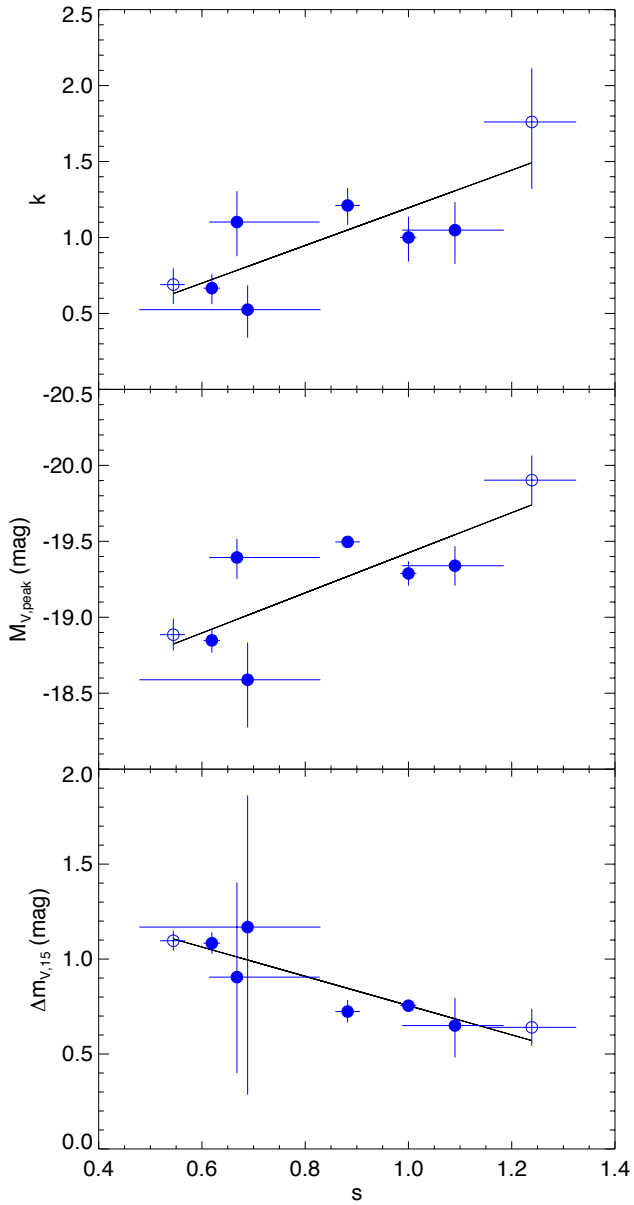


**Fig. 12.** The relations between the  $s$  factor, the  $k$  factor, the decline rate  $\Delta m_{V,15}$  and the peak magnitude  $M_{V,\text{peak}}$ . The best linear fits are plotted in black.

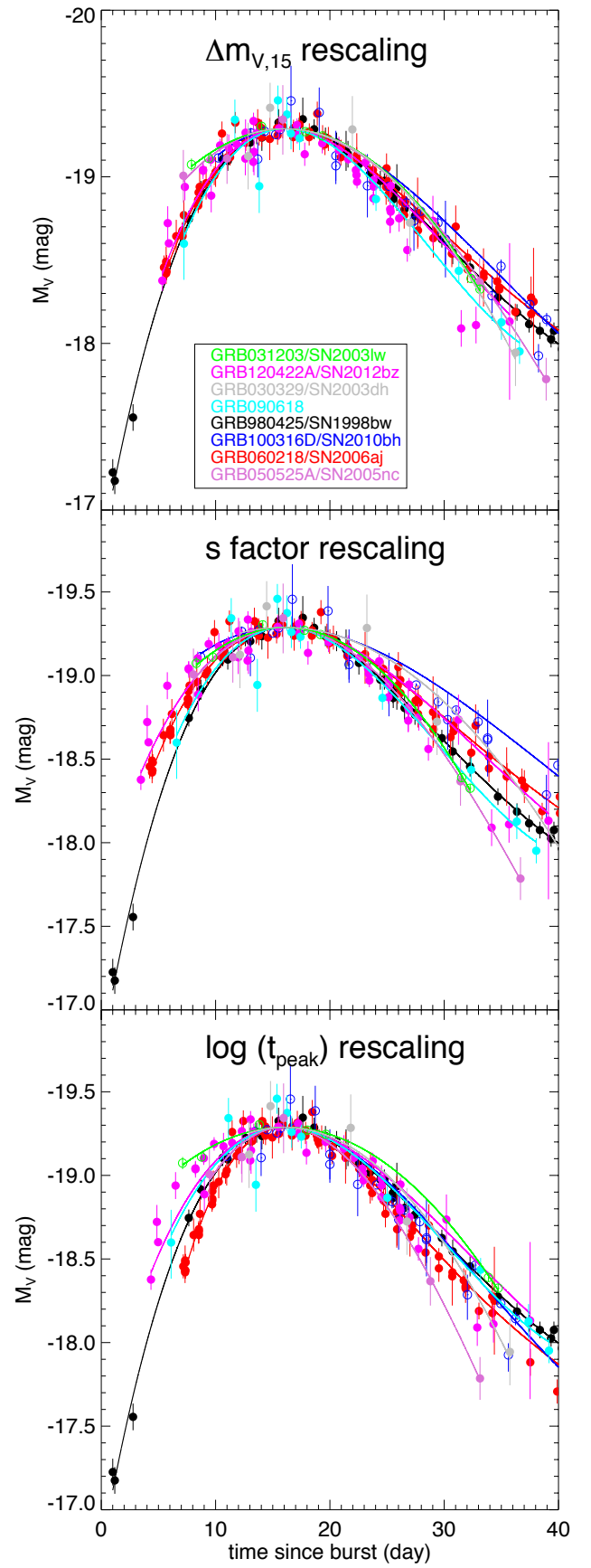


**Fig. 13.** Different rescaling results of the the light curves of the selected systems in rest frame V band. Here  $M_{V,\text{peak}}$  has been normalized to that of SN 1998bw.



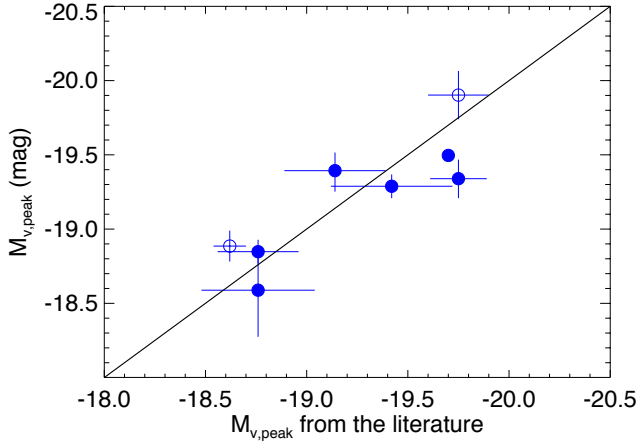


**Fig. 14.** Comparison of the peak magnitudes determined in this paper ( $y$ -axis) and the values from Malesani et al. (2004); Cano et al. (2011a,b); Cano (2013); Schulze et al. (2014) ( $x$ -axis). The illustrative straight line in black is:  $y = x$ . Three outliers are: GRB 090618, XRF 100316D/SN 2010bh and GRB 120422A/SN 2012bz.

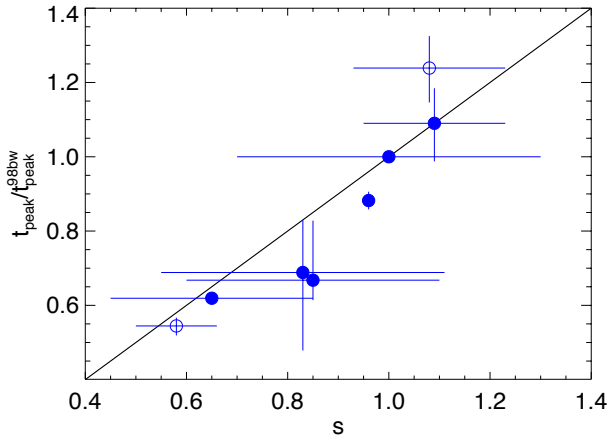


**Fig. 15.** Comparison of peak time  $t_{\text{peak}}$  obtained in this paper (in Table 4) and the stretch factor  $s$  from Cano (2013). Here  $t_{\text{peak}}^{98\text{bw}} = 16.09^{+0.17}_{-0.18}$  days. The illustrative straight line in black is  $y = x$ .